BRIGHAM YOUNG UNIVERSITY

GEOLOGY STUDIES

DECEMBER 1984

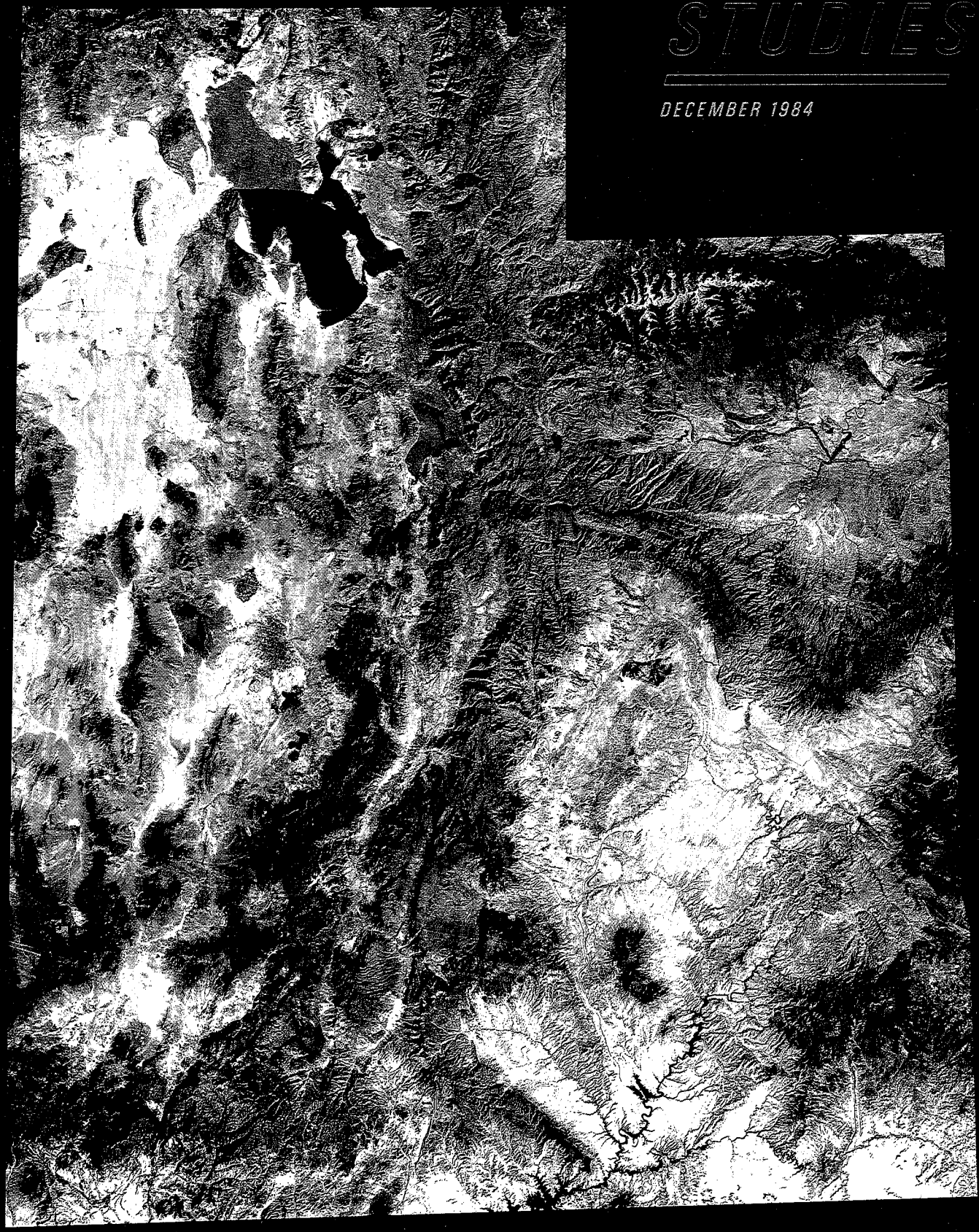

VOLUME 31, PART 1

BRIGHAM YOUNG UNIVERSITY GEOLOGY STUDIES

VOLUME 31, PART 1

CONTENTS

Geology of the Northern Canyon Range, Millard and Juab Counties, Utah ..... John C. Holladay 1

Depositional Environment of the Iron Springs Formation, Gunlock, Utah ..... Brad T Johnson 29

Shnabkaib Member of the Moenkopi Formation: Depositional Environment and Stratigraphy near Virgin, Washington County, Utah ..... Ralph E. Lambert 47

Geology of the Mount Ellen Quadrangle, Henry Mountains, Garfield County, Utah ..... Loren B. Morton 67

Depositional Environments and Paleoecology of Two Quarry Sites in the Middle Cambrian Marjum and Wheeler Formations, House Range, Utah ..... John C. Rogers 97

Carbonate Petrology and Depositional Environments of Carbonate Buildups in the Devonian Guilmette Formation near White Horse Pass, Elko County, Nevada ..... Stephen M. Smith 117

Geology of the Steele Butte Quadrangle, Garfield County, Utah ..... William W. Whitlock 141

Petrography and Microfacies of the Devonian Guilmette Formation in the Pequop Mountains, Elko County, Nevada ..... Winston L. Williams 167

A Geologic Analysis of a Part of Northeastern Utah Using ERTS Multispectral Imagery ..... Robert Brigham Young 187

Publications and Maps of the Department of Geology 213

A publication of the
Department of Geology
Brigham Young University
Provo, Utah 84602

Editors

W. Kenneth Hamblin
Karen Seely

Brigham Young University Geology Studies is published by the Department of Geology. This publication consists of graduate student and faculty research within the department as well as papers submitted by outside contributors. Each article submitted by BYU faculty and outside contributors is externally reviewed by at least two qualified persons.

Cover: LANDSAT Mosaic of the State of Utah. Fall 1976. U.S. Department of Agriculture, Agricultural Stabilization and Conservation Service. Salt Lake City, Utah: Aerial Photography Field Office.

ISSN 0068-1016
Distributed December 1984
12-84 600 74358

CONTENTS

Geology of the Northern Canyon Range, Millard and Juab Counties, Utah, by John C. Holladay 1
Abstract 1
Introduction 1
Location and accessibility 2
Field and laboratory methods 2
Previous work 3
Stratigraphy 3
Precambrian System 3
Pocatello Formation 5
Lower shale member 5
Middle quartzite member 5
Upper shale and siltstone member 5
Blackrock Canyon Limestone 7
Caddy Canyon Quartzite 7
Inkom Formation 7
Mutual Formation 7
Lower member 8
Upper member 8
Cambrian System 8
Cambrian System—Canyon Range allochthon 9
Tintic Quartzite 9
Pioche Formation 9
Howell Limestone 10
Chisholm Formation 10
Dome Limestone 10
Whirlwind Formation 10
Swasey Limestone 10
Wheeler Shale 10
Undivided Cambrian carbonates 10
Cambrian System—Pavant allochthon 11
Tintic Quartzite 11
Pioche Formation (?) 11
Undivided Cambrian carbonates 11
Ordovician System 11
Pogonip Group 11
Cretaceous and Tertiary Systems 11
Canyon Range Formation 13
Lower member 13
Middle member 13
Upper member 15
Red beds of Wide Canyon 15
Fool Creek Conglomerate 15
Oak City Formation 15
Quaternary System 16
Structural geology 16
Thrust faults 16
Canyon Range thrust fault (eastern exposure) ... 16
Canyon Range thrust fault (western exposure) .. 16
Canyon Range thrust fault east of Oak City 16
Syncline axis thrust 19
Folds 19
Canyon Range syncline 19
Canyon Range anticline 20
Tertiary folds 20
Normal faults 21
Bridge Canyon fault 21
Dry Fork fault 21
Wide Canyon–east border fault 21
Recent faults 21
Tear faults 22
Limekiln Canyon fault 22
Syncline axis fault 22
Cow Canyon fault 23
Pavant allochthon 23
Correlation with exposures in the Pavant Mountains 23
Canyon Range thrust footwall ramp 23
Structural evolution of the Canyon Range 24
Overview 24
Directions of thrust movements 25
Magnitudes of thrust displacement 25
Leamington Canyon fault 25
Salt tectonism 26
Economic geology 26
Conclusions 27
Acknowledgments 27
References cited 27
Figures
1. Index map of northern Canyon Range 2
2. Stratigraphic column of Canyon Range allochthon 4
3. Stratigraphic column of Pavant allochthon 5
4. Outcrop of middle member of Pocatello Formation 6
5. Precambrian facies cross section 6
6. Outcrop of upper member of Pocatello Formation 7
7. Outcrop of Blackrock Canyon Limestone 8
8. Geological map of northern Canyon Range in pocket
9. Strike valley eroded along Inkom Formation 9
10. Middle Cambrian stratigraphy of Canyon Range and Pavant allochthons 12
11. Topographic profile of middle member of Canyon Range Formation 14
12. Canyon Range Formation folded in syncline axis 14
13. Structural evolution of Canyon Range 17
14. Eastern exposure of Canyon Range klippe 18
15. Western exposure of Canyon Range klippe 18

16. Canyon Range thrust east of Oak City 19
17. Structural cross sections 20
18. Overturned anticline at Mahogany Hollow 21
19. Tertiary folds of northern Canyon Range 22
20. Canyon Range allochthon subthrust surface 24
21. Geological map of Canyon Range area 26

Depositional Environment of the Iron Springs Formation, Gunlock, Utah, by Brad T Johnson 29
Abstract 29
Introduction 29
General statement 29
Location 29
Previous work 30
Methods 30
Acknowledgments 30
Geologic setting 31
Nomenclature 31
Age 31
Paleogeography 32
Geologic history 32
Stratigraphy 33
Sandstone facies 33
Shale facies 35
Conglomerate facies 35
Red siltstone facies 36
Silty shale facies 36
Dakota Conglomerate 36
Measured sections 37
Provenance 38
Depositional environment 39
Depositional model 40
Summary 43
References cited 43
Appendix A 45
Appendix B 46
Figures
1. Index map 30
2. Detail of measured sections 31
3. Tectonic setting 32
4. Detail of tectonic setting 32
5. Generalized stratigraphic column 34
6. Laminated sandstone 34
7. Deformation in sandstone 34
8. Cross-bedding 34
9. Histogram of sieve data from sandstone 35
10. Shale facies and deformation 35
11. Conglomerate facies 36
12. Red siltstone facies 36
13. Silty shale facies 37
14. Interbedded silty shale and sandstone 37
15. Wavy bedding 37
16. Dakota conglomerate 38
17. Detailed stratigraphic column 39
18. Iron Springs compared to Donjek and Platte Rivers 41
19. Depositional model 42

Shnabkaib Member of the Moenkopi Formation: Depositional Environment and Stratigraphy near Virgin, Washington County, Utah, by Ralph E. Lambert 47
Abstract 47
Introduction 47
Location 48
Methods of study and nomenclature 48
Field methods 48
Laboratory methods 48
Nomenclature 48
Regional setting 48
Previous work 49
Acknowledgments 50
Lithologies 50
Clastic rocks 50
Ripple-laminated siltstone 50
Structureless or horizontally stratified siltstone and siliceous mudstone 50
Chemical precipitates 51
Gypsum 51
Bedded gypsum 51
Nodular gypsum 51
Replacement or secondary gypsum 51
Laminated gypsum 51
Limestone and dolomite 55
Accessory minerals 55
Sedimentary structures 56
Ripple marks and bedding 56
Desiccation cracks 58
Soft-sediment deformation 58
Paleontology 58
Paleoenvironment 59
Paleoclimate 59
Salinity 60
Water energy 60
Lithologic associations 60
Direction of transgression 60
Basin slope 61
Water depth 61
Sedimentary model 62
Supratidal environment 63
Intertidal environment 63
Subtidal environment 63
Summary 63
References cited 64
Figures
1. Index map 48
2. Outcrop of Shnabkaib 49

3. Stratigraphic sections 52, 53
4. Photomicrograph: lenticular bedding 54
5. Outcrop showing gypsum nodules 54
6. Photomicrograph: secondary gypsum crystals ... 54
7. Outcrop of laminated gypsum 54
8. Photomicrograph: algal laminated gypsum 55
9. Photomicrograph: peloidal oolitic wackestone . 56
10. Photomicrograph: oolitic grainstone with radial features 56
11. Photomicrograph: intra-oolitic peloidal wackestone 56
12. Pyritic siltstone 56
13. Wavy lenticular bedding, mottled bedding, and possible ball-and-pillow structure 57
14. Outcrop showing mudcracks 59
15. Deformed bedding 59
16. Fossils 59
17. Fence diagram showing lithologic percentages . 61
18. Depositional model 62

Tables

1. Comparison of ripple mark morphology with McKee 58
2. Comparison of sections 6 and 8 61

Geology of the Mount Ellen Quadrangle, Henry Mountains, Garfield County, Utah, by Loren B. Morton 67
Abstract 67
Introduction 67
Location and accessibility 67
Methods 67
Acknowledgments 68
Previous work 68
Stratigraphy 68
General statement 68
Jurassic System 70
Entrada Sandstone 70
Curtis Formation 70
Summerville Formation 70
Morrison Formation 72
Salt Wash Member 72
Brushy Basin Member 73
Cretaceous System 73
Cedar Mountain Formation 73
Buckhorn Conglomerate Member 73
Upper unnamed shale member 74
Dakota Sandstone 74
Mancos Shale 75
Tununk Shale Member 75
Ferron Sandstone Member 75
Blue Gate Shale Member 76
Muley Canyon Sandstone Member 77
Masuk Shale Member 78
Tertiary System 78
Diorite porphyry 78
Shatter zone 79
Quaternary System 79
Pediment gravels 79
Colluvium 80
Alluvium 80
Landslide debris 80
Talus 80

Structural geology 80
General statement 80
History of laccolithic concepts in the Henry Mountains 80
Gilbert 80
Hunt, Averitt, and Miller 81
Intrusions 81
Stocks 81
Laccoliths 81
South Creek laccolith 81
Dugout Creek laccolith 83
Bysmaliths 86
Ragged Mountain bysmalith 86
Pistol Ridge bysmalith 87
Other Intrusions 88
Laccolith west of Slate Flat 88
North Summit Ridge intrusions 88
Structures that imply other intrusions at depth 89
Faults west of the Pistol Ridge bysmalith 89
Structures west of South Creek Ridge 89
Subsurface information 90
Interpretations 90
Genesis of intrusions 90
Intrusive forms 91
Brittle deformation 91
Confining pressures 91
Economic geology 92
Coal 92
Petroleum 92
Metals 93
Gravels 93
Water resources 93
Summary 93
References cited 94

Figures

1. Index map 68
2. Stratigraphic column 69
3. Bedrock geologic map of the Mount Ellen Quadrangle 71
4. Entrada, Curtis, Summerville, and Salt Wash Members of the Morrison Formation 72
5. Entrada, Curtis, Summerville Formations 72
6. Salt Wash and Brushy Basin Members of the Morrison Formation and Buckhorn Con-

glomerate Member of the Cedar Mountain Formation 73
7. Buckhorn Conglomerate 74
8. Ferron Sandstone and Blue Gate Shale 76
9. Hummocky stratification of lower Ferron Sandstone 77
10. Quartzite inclusion in diorite porphyry 78
11. Quaternary pediment gravels 79
12. Cross section D–D′ 82
13. Low-angle reverse fault in front of South Creek–Bullfrog laccoliths 83
14. Closeup of overturned Ferron Sandstone 83
15. Cross section of B–B′ 84
16. Slate and slate breccia at Head of Bullfrog dike . 84
17. Dugout Creek laccolith from Star Flat 85
18. Low-angle reverse fault in front of Dugout Creek laccolith 85
19. Dugout Creek laccolith 85
20. Cross section C–C′ 86
21. Cross section E–E′ 87
22. Pistol Ridge bysmalith 88
23. Rotated block of Salt Wash Member 89
24. Perpendicular-type normal faults 90
25. Ferron coal outcrop 92

Depositional Environments and Paleoecology of Two Quarry Sites in the Middle Cambrian Marjum and Wheeler Formations, House Range, Utah, by John C. Rogers 97
Abstract 97
Introduction 97
Location 98
Swasey Spring site 98
Sponge Gully site 98
Methods of study 98
Previous work 98
Stratigraphy 100
Swasey Limestone 100
Wheeler Shale 100
Marjum Formation 100
Weeks Limestone 100
Sponge Gully quarry 100
Lithology 101
Graded bedding 101
Soft-sediment folds 101
Low-angle truncations 101
Oriented fossils 104
Fragmented organic debris 105
Tool marks, sole marks, and microscopic scouring 105
Depositional model 105
Paleoecology 109
Paleontology 109
Swasey Spring quarry 110
Lithology 110
Graded bedding 110
Soft-sediment folds 111
Low-angle truncations 111
Oriented fossils 111
Fragmented organic debris 111
Tool marks, sole marks, and microscopic scouring 111
Depositional model 112
Paleoecology 113
Paleontology 113
Conclusion 113
Acknowledgments 114
References cited 114
Figures
1. Index map 97
2. Swasey Spring quarry 98
3. Sponge Gully quarry 98
4. House embayment 98
5. House Range stratigraphic column 99
6. Lithologies, orientation, and abundance of organisms in the quarries 102
7. Photomicrograph: shale in Marjum Fm. at Sponge Gully 103
8. Photomicrograph: limestone in Marjum Fm. at Sponge Gully 103
9. Photomicrograph: distribution grading 103
10. Photomicrograph: graded peloids 103
11. Soft-sediment fold 103
12. Trend of basin from movement of slumps 104
13. Low-angle truncations 104
14. Large-scale gravity slide 104
15. Small-scale gravity slide 104
16. Oriented *Yuknessia* 105
17. Orientation of organisms at Sponge Gully 106
18. Block diagram: depositional model 107
19. Westward migration of carbonate bank 107
20. Sponge Gully specks 108
21. Tool marks 108
22. Sole marks 109
23. Trace fossils 109
24. Photomicrograph: shale in Wheeler Shale at Swasey Spring 110
25. Photomicrograph: limestone in Wheeler Shale at Swasey Spring 110
26. Orientation of organisms at Swasey Spring 112
27. Swasey Spring specks 113

Carbonate Petrology and Depositional Environments of Carbonate Buildups in the Devonian Guilmette Formation near White Horse Pass, Elko County, Nevada, by Stephen M. Smith 117
Abstract 117

Introduction 117
Location 117
Methods and nomenclature 117
Previous work 118
Acknowledgments 119
Geometry and carbonate petrology of lithofacies 119
Lithofacies A 120
Lithofacies B 120
Alternating light and dark dolomite subfacies .. 120
Homogeneous dolomite subfacies 120
Heterogeneous dolomite subfacies 120
Lithofacies C 121
Pelletal packstone/grainstone subfacies 121
Amphipora packstone and wackestone subfacies 121
Pelletal packstone and wackestone subfacies 121
Skeletal packstone and wackestone subfacies ... 125
Peloidal wackestone and mudstone subfacies ... 128
Heterogeneous and homogeneous dolomites 128
Lithofacies D 128
Lithofacies E 128
Pelletal grainstone and packstone subfacies 129
Skeletal pelletal packstone and wackestone subfacies 129
Pelletal packstone and wackestone subfacies 130
Lithofacies F 130
Peloidal-pelletal packstone subfacies 131
Fenestral wackestone and mudstone subfacies .. 131
Sandy dolomite subfacies 131
Lithofacies G 132
Paleontology 132
Diagenesis 133
Recrystallization 133
Dolomitization 134
Depositional environments of carbonate lithofacies 135
Lithofacies A 135
Lithofacies B 135
Lithofacies C 136
Pelletal packstone/grainstone subfacies 136
Amphipora packstone and wackestone subfacies 136
Pelletal packstone and wackestone subfacies 136
Skeletal packstone and wackestone subfacies ... 136
Peloidal wackestone and mudstone subfacies ... 136
Heterogeneous and homogeneous dolomites 136
Lithofacies D 136
Lithofacies E 136
Pelletal grainstone and packstone subfacies 136
Skeletal pelletal packstone and wackestone subfacies 137
Pelletal packstone and wackestone subfacies 137
Lithofacies F 137
Peloidal-pelletal packstone subfacies 137
Fenestral wackestone and mudstone subfacies .. 137
Sandy dolomite subfacies 137
Lithofacies G 137
Conclusions 137
References cited 138
Figures
1. Index map 118
2. Classification of carbonate rocks 118
3. Classification of stylolites 119
4. Stratigraphic columns of measured sections 122, 123, 124
5. Laminated character of lithofacies A 125
6. Alternating light and dark "spaghetti" dolomite subfacies 125
7. Closeup of alternating light and dark "spaghetti" subfacies 125
8. "Spaghetti" dolomite 125
9. Stylolites separating light and dark dolomite 126
10. Photomicrograph: xenotopic dolomite 126
11. Replaced stromatoporoids(?) 126
12. Photomicrograph: grainstone/packstone 126
13. Photomicrograph: *Amphipora* encrusted with algae 126
14. Scattered dolorhombs in wackestone fabric 126
15. In situ bulbous stromatoporoids 127
16. Upside-down stromatoporoid biscuit 127
17. Tabular stromatoporoid 127
18. Photomicrograph: *Vermiporella* 127
19. Photomicrograph: prismatic-wall-type calcisphere 127
20. Photomicrograph: spinose-wall-type calcisphere 128
21. Photomicrograph: fenestral fabric 128
22. Prominent exposure of lithofacies E 129
23. Oriented *Stringocephalus* in grainstone 130
24. Photomicrograph: *Stringocephalus* 130
25. Photomicrograph: *Solenopora* 130
26. Felt Wash section 131
27. Photomicrograph: crinoid columnal 132
28. Nautiloid 132
29. Photomicrograph: ostracode clusters 132
30. Photomicrograph: *Amphipora* 133
31. Photomicrograph: *Trupetostroma*(?) 133
32. Photomicrograph: *Hammatostroma*(?) 133
33. Rugose corals 134
34. Photomicrograph: uniserial foraminifera 134
35. Photomicrograph: nodosinelled 134
36. Photomicrograph: endothyrid 134
37. Depositional model 138

Geology of the Steele Butte Quadrangle, Garfield County, Utah, by William W. Whitlock 141
Abstract 141
Introduction 141
Location and accessibility 141

Methods 141
Previous work 142
Acknowledgments 142
Stratigraphy and sedimentation 142
General statement 142
Jurassic System 142
Entrada Sandstone 142
Curtis Formation 144
Summerville Formation 144
Morrison Formation 144
Salt Wash Member 144
Brushy Basin Member 145
Cretaceous System 145
Cedar Mountain Formation 145
Buckhorn Conglomerate Member 145
Upper member 146
Dakota Sandstone 146
Mancos Shale 146
Tununk Shale Member 146
Ferron Sandstone Member 147
Blue Gate Shale Member 148
Muley Canyon Sandstone Member 148
Masuk Shale Member 155
Tarantula Mesa Sandstone 156
"Beds on Tarantula Mesa" 157
Tertiary System 158
Diorite porphyry intrusions 158
Quaternary System 158
Pediment gravel 158
Alluvial terrace gravel 158
Stream alluvium 159
Eolian sand and loess 159
Colluvium 159
Structural geology 159
General statement 159
Henry Mountains structural basin 159
Structures associated with intrusive bodies 159
Toreva-block slides 159
Economic geology 159
Coal 159
Petroleum 163
Construction materials 163
Water resources 163
Summary 163
References cited 164

Figures

1. Index map 142
2. General stratigraphic column 143
3. Exposure of Entrada Sandstone, Curtis Formation, Summerville Formation, and Salt Wash Member of the Morrison Formation 144
4. Exposure of Salt Wash and Brushy Basin Members of the Morrison Formation and Buckhorn Conglomerate Member of the Cedar Mountain Formation 145
5. Exposure of Buckhorn Conglomerate and upper members of the Cedar Mountain Formation and Dakota Sandstone 146
6. Exposure of Tununk Shale Member of the Mancos Shale 147
7. Exposure of Ferron Sandstone and Tununk Shale Members of the Mancos Shale 147
8. Exposure of Blue Gate Shale and Muley Canyon Sandstone Members of the Mancos Shale 148
9. Blue Gate Shale transitional facies 148
10. Stratigraphic column of Muley Canyon Sandstone 149
11. Exposure of Muley Canyon-1 unit 150
12. Exposure of Muley Canyon-2 unit 151
13. Diagram of coal sections 152, 153
14. Exposure of Muley Canyon-3, Masuk Shale-1, Masuk Shale-2, Masuk Shale-3, Tarantula Mesa Sandstone 154
15. Exposure of Muley Canyon-3 cliffs 154
16. Fluvial channel in Muley Canyon-3 unit 155
17. Stratigraphic column of Masuk Shale 156
18. Stratigraphic column of Tarantula Mesa Sandstone 157
19. Cliffs of Tarantula Mesa-1 and Tarantula Mesa-2 158
20. Sandstone lenses in Tarantula Mesa Sandstone .. 158
21. Structural contour map and simplified geologic map 160
22. Coal isopach map and simplified geologic map . 162

Petrography and Microfacies of the Devonian Guilmette Formation in the Pequop Mountains, Elko County, Nevada, by Winston L. Williams 167
Abstract 167
Introduction and location 167
Acknowledgments 167
Previous work 168
Methods 169
Geologic setting 169
Microlithofacies 169
Packstone 170
Uniform Packstone 170
Mixed Packstone 170
Wackestone 170
Uniform Muddy Wackestone 170
Mixed Wackestone 170
Sandstone 171
Stromatolitic Boundstone 172
Dolomite and Dolomitic Units 173
Paleontology 174
Upper Devonian 174
Lower Mississippian 178

Depositional model 178
Diagenesis 182
Economic significance 183
Conclusions 184
References cited 185
Figures
1. Index map 168
2. Main buildup 169
3. Measured sections ..... in pocket
4. Photomicrograph: uniform sparry packstone 170
5. Photomicrograph: uniform muddy packstone ... 171
6. Photomicrograph: mixed sparry packstone 171
7. Photomicrograph: mixed muddy packstone 172
8. Photomicrograph: dolomitic uniform muddy wackestone 172
9. Photomicrograph: mixed sparry wackestone 173
10. Photomicrograph: mixed muddy wackestone 173
11a. Photomicrograph: cross-bedded sand unit 174
11b. Cross-bedded sand unit 174
12. Photomicrograph: stromatolitic boundstone (algal mat) 175
13. Photomicrograph: "correlation" dolomite unit . 175
14a. Photomicrograph: *Stromatopora cygnea* 176
14b. Photomicrograph: *Talaestroma steleforme* 176
14c. Photomicrograph: ?*Trupetostroma* sp. 176
15. Photomicrograph: diastem within a stromatoporoid's coenostea 176
16a. Photomicrograph: calcareous alga ?*Stenophycus* sp. 177
16b. Photomicrograph: calcareous alga ?*Keega* sp. ... 177
16c. Photomicrograph: calcareous alga ?*Litanaia* sp. 177
16d. Photomicrograph: calcareous alga ?*Ortonella* sp. 177
16e. Photomicrograph: calcareous alga ?*Tharama* sp. 177
16f. Photomicrograph: calcareous alga of unknown genus 177
17. SEM photomicrographs: Kinderhookian conodonts from Joana Limestone 179
18. Flanking beds on mound 180
19. Unconformable contact between Guilmette Formation and Joana Limestone 181
20. Long intraclast with possible ghosted isopachous rim 182
21. Idealized depositional model of mound and surrounding shelf sediments 183
22. Strained calcite 184

A Geologic Analysis of a Part of Northeastern Utah Using ERTS Multispectral Imagery, by Robert Brigham Young 187
Abstract 187
Acknowledgments 187
Introduction 187
Objective 187
Location 187
Previous work 187
Methods of investigation 188
Geologic setting 188
General statement 188
Geologic history 190
Phase I 190
Phase II 190
Phase III 190
Phase IV 191
Phase V 191
Phase VI 192
Classification 192
General statement 192
Lineations 192
Lineation distribution 192
Introduction 192
Quadrant description 192
Northwest quadrant 192
Northeast quadrant 192
Southeast quadrant 192
Southwest quadrant 192
Uinta Megalineament 193
Description 193
Structure 194
Geophysics 194
Economics 194
Towanta Megalineament 194
Description 194
Structure 194
Geophysics 194
Economics 195
Strawberry Megalineament 197
Description 197
Structure 199
Geophysics 200
Economics 201
Badlands Cliffs and Book Cliffs Megalineaments .. 201
Badlands Cliffs Megalineament 201
Description 201
Structure 201
Geophysics 201
Economics 201
Book Cliffs Megalineament 201
Description 201
Structure 202
Geophysics 202
Economics 202
Uncompahgre-Raft River Megalineament 202
Description 202
Structure 202
Geophysics 202

Economics 203
Scofield Megalineament 203
Description 203
Structure 203
Geophysics 203
Economics 203
Wasatch East Megalineament 203
Description 203
Structure 204
Geophysics 204
Economics 204
Wasatch West Megalineament 204
Description 204
Structure 204
Geophysics 204
Economics 205
Analysis 205
General statement 205
Computer analysis 205
Linear intersection frequency 205
Linear density 207
Annular structures 207
General statement 207
Summary 207
References cited 209
Figures
1. Index map 188
2. Drainage map with geomorphic provinces 189
3. ERTS Image 5544-16413 190
4. Lineation map 191
5. Megalineaments 193
6. Annular structures 195
7. Tectonic map 196
8. Aeromagnetic map 197
9. Bouguer gravity map 198
10. Recorded seismic activity map 199
11. Economic geology map 200
12. Orientation histogram 205
13. Intersection frequency contour map 206
14. Lineation density contour map 208
Publications and maps of the Department of Geology 213

A Geologic Analysis of a Part of Northeastern Utah Using ERTS Multispectral Imagery*

ROBERT BRIGHAM YOUNG
Amoco Production Company, Houston, Texas 77042

Thesis chairman: JAMES L. BAER

ABSTRACT

A study area encompassing approximately 11,230 km² in northeastern Utah has been analyzed using multispectral ERTS imagery. Six hundred fifty-one linears and 116 associated annular structures have been identified. Nine megalineaments (over 100 km long) are present in the area, and their mutual intersections appear to be important controls of mineralization and petroleum accumulation possibly facilitated by intersection generated fracture permeability. Comparison of linear patterns and geophysical data indicate four separate tectonic blocks within the study area. A histogram of lineation trends compared with earlier studies provides favorable evidence for regional control of major linear trends in the Colorado Plateau and the Uinta-Wasatch transition zone.

ACKNOWLEDGMENTS

I wish to express my sincere gratitude to all those who have helped me in making this thesis possible.

Special appreciation is extended to my fellow graduate students for their kind and considerate willingness to act as my "sounding board" and for the resulting thought-stimulating discussions.

Acknowledgment of the entire Brigham Young University geology faculty is also appropriate, for I was never turned from a door unaided. I am indebted to Drs. Kenneth Bullock and Dana Griffen for their critical reading of the text and to Dr. Wm. Revell Phillips for serving on my committee. To Dr. James L. Baer, I extend heartfelt thanks for his very competent chairmanship of my committee. Although difficulties beyond my control prolonged the preparation of this thesis, he was unfailingly kind, helpful, and understanding.

The most special gratitude of all is reserved for my wife and children for their indulgence and help in this effort.

INTRODUCTION

OBJECTIVE

The objective of this study is to discern and interpret the geologic significance of several major and minor linear features found in the study area (fig. 1). The study of these linear features is based upon a correlation of geophysical, geomorphic, economic, and structural data.

LOCATION

The study area is an approximately 11,230-square-kilometer tract located in northeastern Utah (fig. 1). The study area contains portions of the following major physiographic units: the Middle Rocky Mountains, the Colorado Plateau, and the Basin and Range.

Thirteen geomorphic subdivisions of Utah (Stokes 1977) are represented in the study area (fig. 2). They include the Uinta Mountains, the Wasatch hinterland, the Wasatch Range, the Wasatch Front valleys, the Book Cliffs-Roan Plateau section, the Wasatch Plateau, and the Uinta Basin. Present, in part, are the Gunnison Plateau-Valley Mountains section, the Pavant Range-Canyon Range section, the Sanpete-Sevier Valley section, and the Mancos Shale lowland.

PREVIOUS WORK

Many papers have been published concerning the study area, but only a few are pertinent to this study. These include the following: Gallacher (1975) presented a report "Fractures and Surface Lineaments in Northeastern Utah." A study utilizing lineament analysis to define structural and stratigraphic anomalies was published by

*A thesis submitted to the Department of Geology, Brigham Young University, in partial fulfillment of the requirements for the degree Master of Science, December 1980.

Johnson in 1976. Levandowski and others (1976) studied lineaments and aeromagnetic anomalies and their relationships to the geologic structure of north central Nevada. Taranik and Trautwein (1976) discussed the integration of geologic remote-sensing techniques (mostly multispectral Landsat data) with subsurface analysis. Peterson (1976) presented an analysis of curvilinear features detected from Landsat imagery as a method for defining probable areas of high fracture porosity and permeability. Johnson (1976) reported a comparable study of a different area. Ritzma (1976) discussed the Towanta Lineament in northeastern Utah. Erickson (1976) discussed the economic importance of the Uinta-Gold Hill trend. Smith (1976) mapped arcuate surface patterns (curvilinears) in the southwestern United States. Salas (1977) reported on the relationships of linear features to mineral resources in Mexico, using multispectral Landsat data. The tectonic history and structure of the Indianola Quadrangle was treated by Runyon (1977). Taranik (1978) wrote two useful papers: one dealing with the characteristics of the Landsat multispectral scanning system and the other treating computer processing of Landsat data for geologic applications.

METHODS OF INVESTIGATION

NASA ERTS image 5544-16413 (fig. 3), acquired by Landsat-2 on 14 October 1976, was selected for this study because essentially no cloud cover is displayed. Topographic features, because of low sun angle, are displayed with excellent contrast. Black and white prints (185 mm × 185 mm, 1:1,000,000 scale) in each of the four available bands (band 4, green; band 5, red; band 6, near infrared; and band 7, near infrared) along with black and white positive transparencies (185 mm × 185 mm, 1:1,000,000 scale) in each of the four bands were obtained. False color composite images, which are prepared by exposing three of the four black and white bands through different color filters onto color film are also available. A 530 mm × 530 mm, 1:365,000 scale false color composite print (bands 4, 5, and 7) was also used. A smaller scale (1:1,000,000 scale) false color composite negative transparency in the 185 mm × 185 mm size was also used.

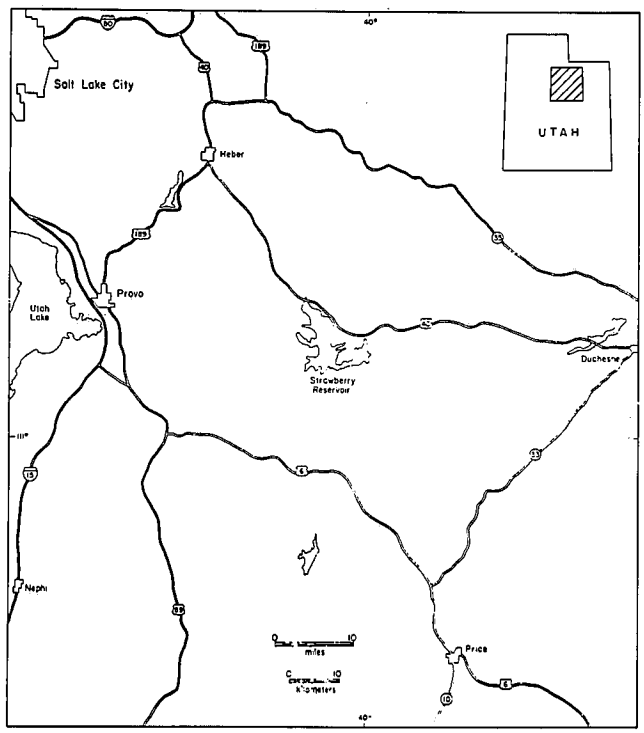

FIGURE 1.—*Index map of the study area illustrating the Wasatch-Uinta transition zone and surrounding area.*

Skylab photographs, 83-301, 83-302, and 83-303, taken from an altitude of 430 km were used for a part of the study area. These photographs cover a large portion of the study area and were especially useful because overlapping coverage gave opportunity for stereoscopic examination. Only a small portion of the northwest corner of the study area was not studied stereoscopically using satellite imagery.

Transparencies in each of the four black and white bands and the false color composite negative transparency were projected onto a screen using an overhead projecter. Linears, lineaments, megalineaments (figs. 3, 5) and annular features (fig. 6) were noted. Black and white prints in each of the four bands were examined on a light table. The light table was also used in the examination of the false color composite print. Examination of band 7 in both the transparencies and the prints was the most informative.

A lineation map (fig. 4) was prepared from the synthesis of information from each image excluding all linears less than 4 km in length. This was compared with the lineation map created from the false color composite print alone. Excellent correlation was noted. This lineation map was compared with structural, tectonic, geomorphic, geophysical, and economic data. Analysis of lineation trends, length, and intersection frequency was performed. A histogram of lineation trend was prepared (fig. 12). Data of lineation intersection frequency and lineation density were computer processed utilizing the SYMAP program in an IBM 360, resulting in machine-generated contour maps (figs. 13, 14).

GEOLOGIC SETTING

GENERAL STATEMENT

The geologic and tectonic history of the study area is a complicated aggregate of events profoundly influenced

by tectonic events along the nearby Wasatch-Las Vegas hingeline. This persistent geologic feature is traced in Utah from southwestern to northern Utah near the Wyoming border and has controlled sedimentation, via a yoked relationship, on either side of it. The study area lies east of this hingeline.

The area has been the locus of numerous multi-directional forces. Tectonic features of several major orogenic pulses have overprinted the area. They include the Cordilleran geosyncline, the ancestral Rocky Mountains, the Sevier orogeny, the Laramide orogeny, formation of the Green River and Flagstaff Lakes, Oligocene intrusive

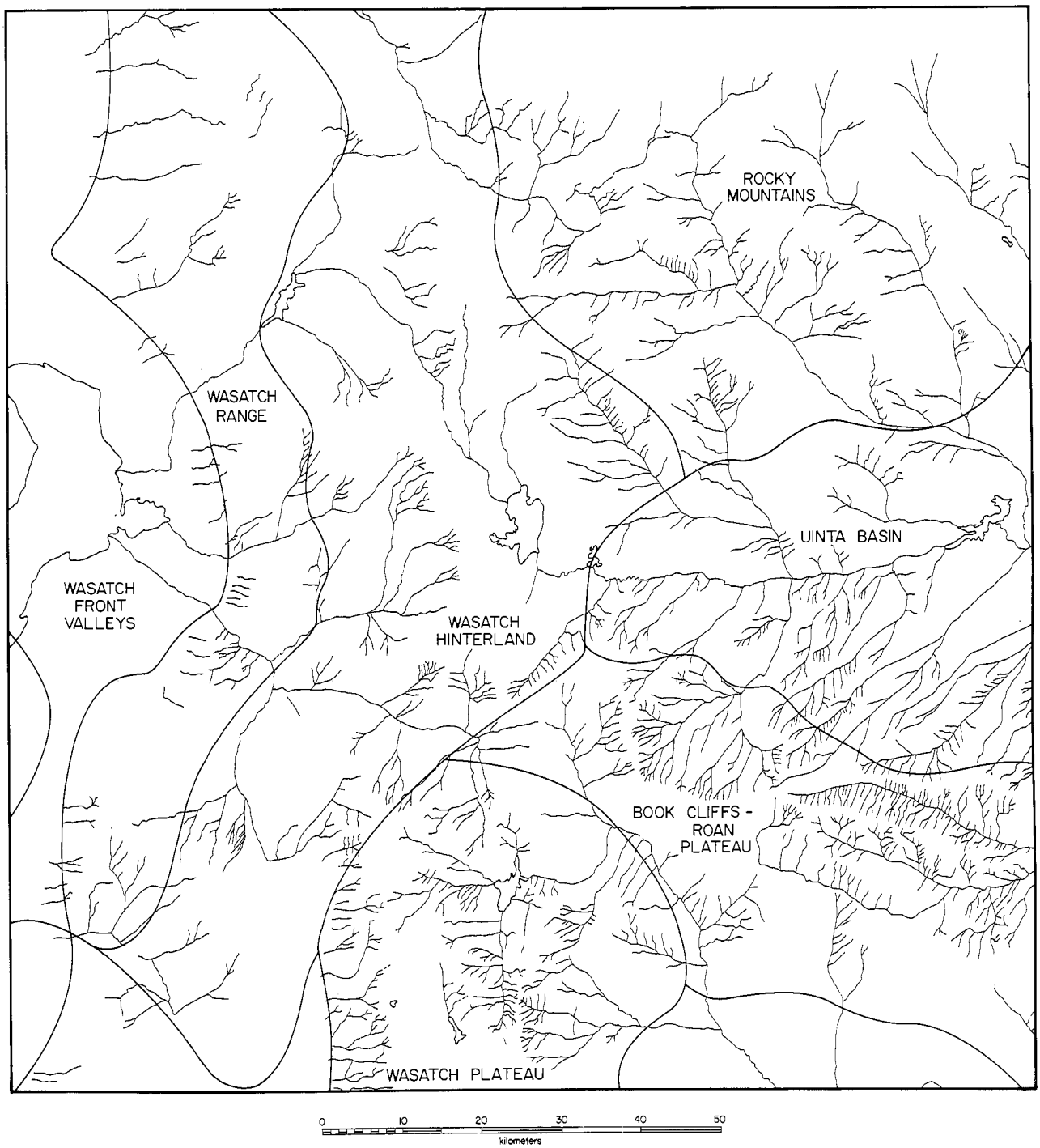

FIGURE 2.—*Drainage map with geomorphic provinces (adapted from Stokes 1977).*

and extrusive episodes, and Miocene to Recent taphrogenic events. Many surface features of these events remain uninterpreted.

GEOLOGIC HISTORY

Hintze (1973) divides Utah geologic history into six phases.

Phase I

During Precambrian to Devonian time, the study area was situated in a shallow-marine environment, not unlike the Bahamas Bank of today.

Phase II

From Mississippian to Early Triassic, a reversal in sedimentation direction occurred, with concomitant formation of deeply subsiding marine basins and adjacent uplifts. The Oquirrh Basin and the Uncompahgre Uplift of this period are important structures in the study area.

Phase III

The Late Triassic to early Cenozoic phase saw the Sevier orogenic belt shedding sediments eastward into marine and nonmarine depositional basins and represents a

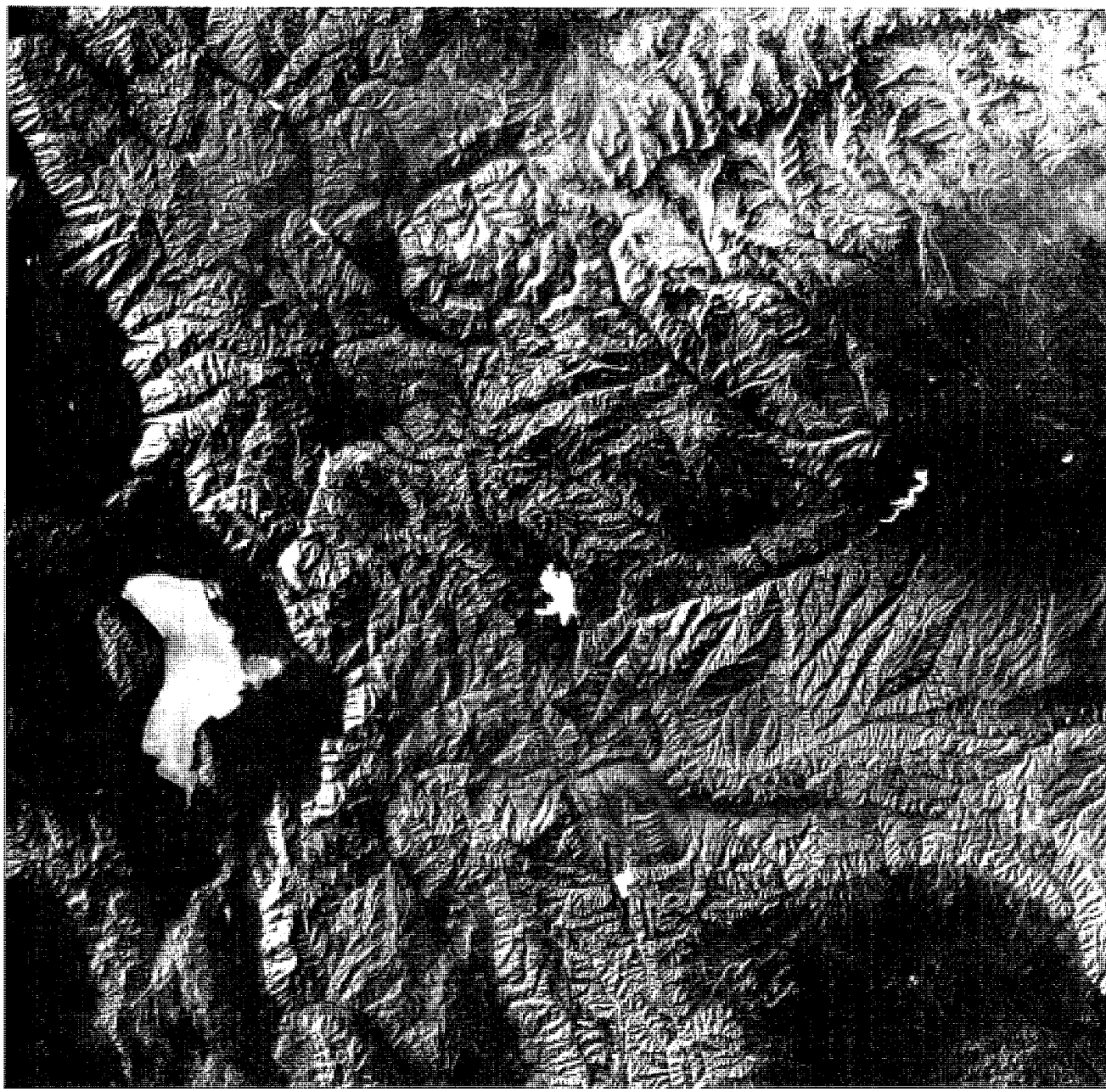

FIGURE 3.—*ERTS image 5544-16413, covers all of study area and surrounding areas. Utah Lake is in the west central portion.*

complete reversal of sedimentation from Phase I. The Uncompahgre Uplift continued to rise and extended its influence to the northwest via the Northern Utah Arch, at least as far as the Raft River Mountains in northwest Utah (Heylman 1959).

Phase IV

From Late Cretaceous to Eocene, high-angle faulting and uplift of the Laramide orogeny occurred. It included the rise of the Uinta Arch and the accompanying subsidence of the Uinta Basin wherein thousands of meters of stream and lake deposits accumulated.

Phase V

Volcanic centers of Phase V affected much of Utah. Oligocene intrusives and extrusives are present in the western portion of the study area.

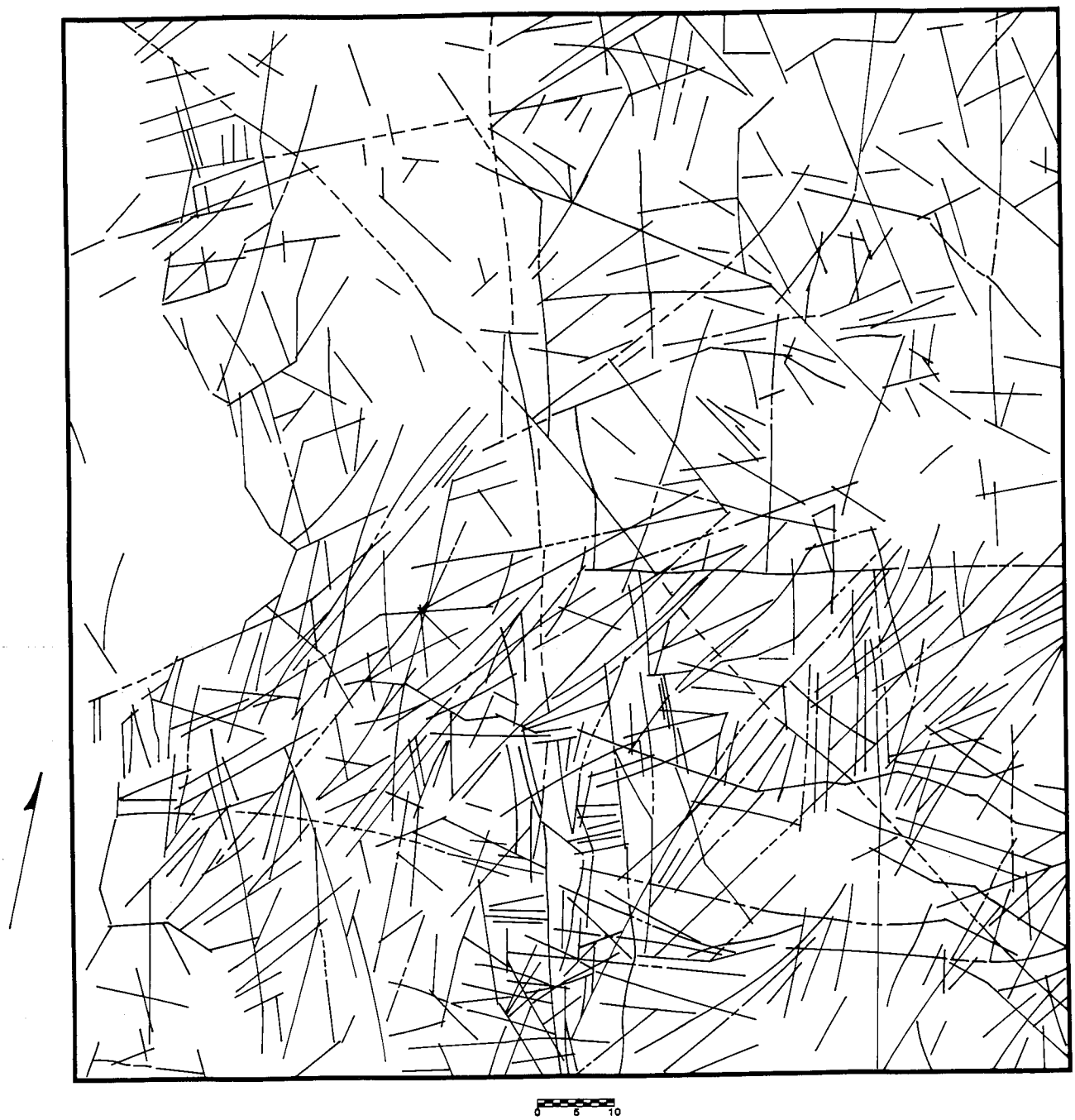

FIGURE 4.—*Lineation map.*

Phase VI

The Miocene to Recent phase is characterized by block faulting along the western margin of the study area, regional uplift, nonmarine sediments, and glaciation of the flanks of the Uinta and Wasatch Mountains. A profound influence on the topography of the area has been exerted by the regional uplift of the Colorado Plateau.

CLASSIFICATION

GENERAL STATEMENT

Historically, linear features recognized on the earth's surface have intrigued geologists. Hodgeson (1976) provides, for those interested, a complete and informative review of the early study of lineations. With the advent of satellite imagery, a new scale of observation is accessible for the study of linear features. Many geologists have been quick to utilize this new tool. As with any new field, nomenclature difficulties have arisen with many words seeming to have as many definitions as users. Sensing a need for clarity, I have defined the terms of this report, using the excellent terminology proposed by El-Etr (1976).

Linear: A descriptive and nongenetic term for any lineation within or on a rock, exposed or covered by surficial material, less than 10 km long.

Lineament: A descriptive and nongenetic term for any lineation within or on a rock, exposed or covered by surficial material, 10–100 km long.

Megalineament: A descriptive and nongenetic term for any lineation more than 100 km long.

When I refer to linear features generically, the term *lineation* will be used.

In the study area, a feature not covered by El-Etr's definitions was recognized. A substantial number of circular to ellipsoidal features of various sizes were seen. *Annular structure* is the term chosen for those features. They are not differentiated according to size. *Annular structure* is defined as a descriptive, nongenetic term for any circular or ellipsoidal feature within or on a rock exposed or covered by surficial material.

LINEATIONS

LINEATION DISTRIBUTION

Introduction

Examination of the lineation map (fig. 4) reveals the following: (1) Nine megalineaments (fig. 5), which will be described and discussed singly later, are recognized; (2) lineation patterns vary with location in the study area (fig. 4); (3) occurrences of lineations are conspicuously more prevalent in the southern half of the study area (figs. 4, 5). The study area is divided into roughly equal area quadrants (figs. 4, 5) by the Scofield (north-south trend) and the Strawberry (east-west trend) Megalineaments (fig. 5). In each of the four quadrants derived by the intersection of these two megalineaments is a distinctive characteristic which delineates each quadrant. Each quadrant displays a different lineation pattern, which results from variations in lineation trend and density (fig. 4).

QUADRANT DESCRIPTION

Northwest Quadrant

Lineations are largely confined to the Wasatch Mountains (fig. 4), and the majority display a pronounced northwestward bias. Large areas of the quadrant are void of lineations, probably because of cultural features and land cultivation masking the lineation trends. The intersection of the Uinta, Wasatch East, and Uncompahgre-Raft River Megalineaments is associated with an economically important mineralized area in this quadrant.

Northeast Quadrant

Distribution of lineations is more uniform in the northeast quadrant (fig. 4), and their density is comparatively greater. No dominant trend is readily observed. The Uinta Megalineament is present (fig. 5) but does not intersect any other megalineament. A major zone of intersection does occur in the quadrant involving the Towanta, Scofield, and Uncompahgre-Raft River Megalineaments (fig. 5).

Southeast Quadrant

Density of lineations is much greater in this quadrant than in the previous two (fig. 4), with north-south, east-west, and northeast-southwest trends being about equally represented. Even though the largest linear feature in the study area, the northwest-trending Uncompahgre-Raft River Megalineament (fig. 5), passes through the quadrant, there is a noticeable scarcity of other northwest lineations.

Southwest Quadrant

Except for the extreme northwest corner of the quadrant (Utah Valley), lineation population is more dense and more regularly distributed than in the previous three (fig. 4) with northeast trends strongly dominant. Three zones of major intersection of megalineaments are observable (fig. 5) involving the curved west limb of the Strawberry, the Book Cliffs, the Bad Lands Cliffs, the Wasatch East, and the Wasatch West Megalineaments.

UINTA MEGALINEAMENT

Description

The Uinta Megalineament is a major east-west-trending feature (fig. 2, 3, 5) which is traced for 124 km across the study area with an average trend of 77°. The megalineament's termini are uncertain, but Erickson (1976) indicates that the Uinta Megalineament may be traced from eastern Nevada through Utah into western Colorado. In the study area, the megalineament is initially expressed as the crest of the west dome of the Uinta Mountains and is traced westward from the vicinity of Kings Peak to a brief

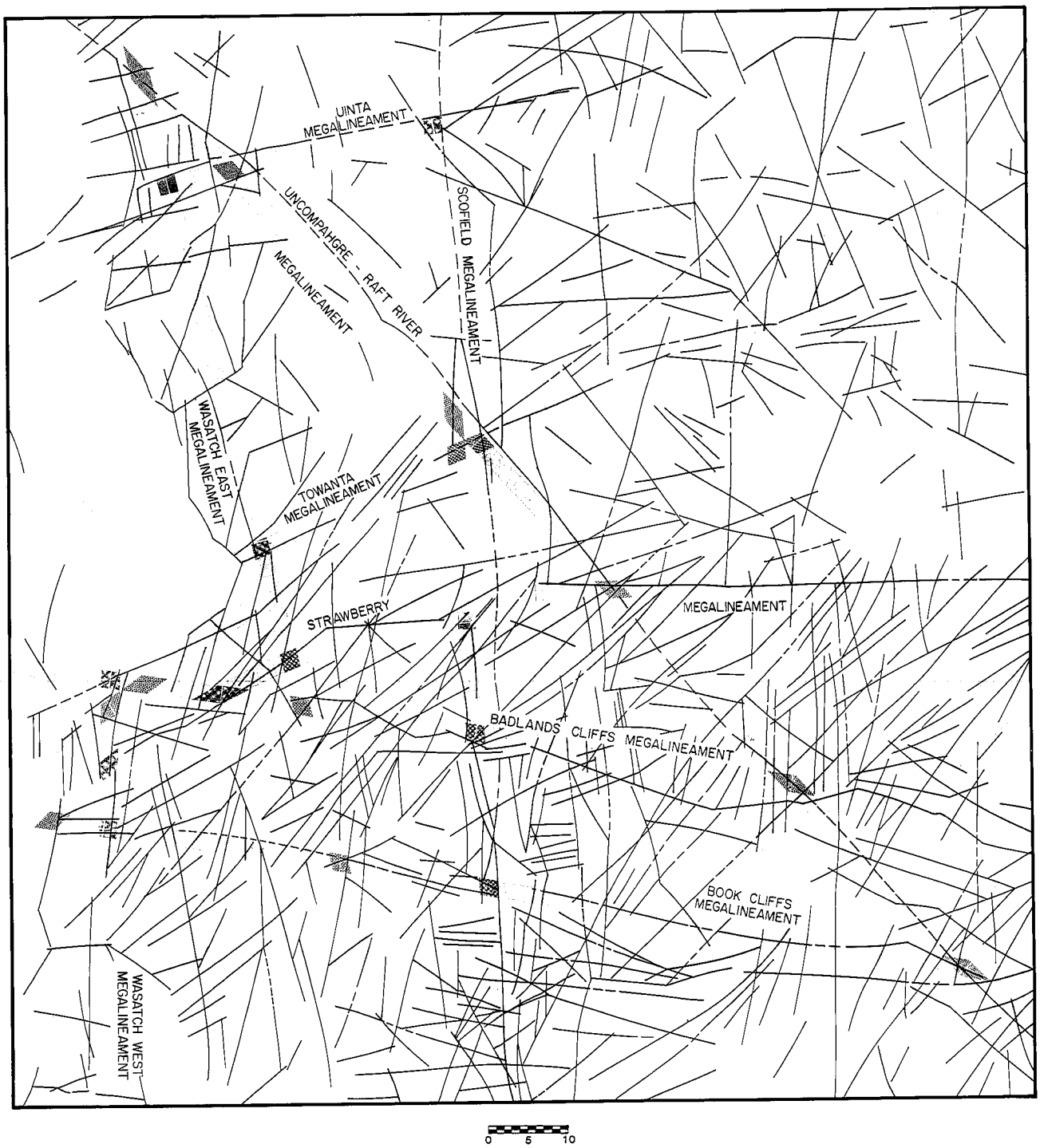

FIGURE 5.—*Lineation map with superimposed megalineaments.*

interruption at Kamas Plain (fig. 5). Resumption of the megalineament, west of Kamas, is defined by albedo patterns and alignments of small ridges and valleys which blend into the Traverse Mountains at the western border of the study area.

Structure

East-west faults are common in the western Uinta Mountains (fig. 7) and are essentially parallel to the Uinta Megalineament. Near the western margin of the Uinta Mountains, fault density decreases noticeably. An annular structure (fig. 6) overprints the west-plunging nose of the west dome of the Uinta Mountains and appears to control this decrease in fault density. Fault density increases in the Tertiary volcanics west of Kamas Plain and continues, but with increasing divergence westward, only somewhat parallel to the megalineament. An abrupt change occurs west of the boundary fault of the Little Cottonwood Stock where fault trends rotate approximately 90° to a north-south direction (fig. 7). This change appears where the megalineament enters the Basin and Range Province, in which north-south blockfaulting is a definitive characteristic.

Geophysics

An east-west-trending alignment of aeromagnetic highs (fig. 8) which degenerate to an east-plunging aeromagnetic ridge substantially follows the Uinta Megalineament (Zietz 1976, Mabey and others 1964). A gravity ridge (fig. 9), plunging slightly south of west (Cook and others 1975), also aligns well with the trend of the megalineament. A scanty seismic pattern correlates well with the megalineament (fig. 10); however, the evidence is inconclusive (Arabasz and others 1979). Basement maps prepared by Condie (1969; fig. 7) indicate the Uinta Megalineament lies within the Churchill Basement Province (1.6 to 1.8 b.y.b.p.) of which the Uinta Subprovince is a subdivision and which is elongate east-west. Near the western margin of the Uinta Subprovince this east-west trend bifurcates yielding northwest- and southwest-trending forks. The Uinta Megalineament follows approximately the centerline of the east-west trend of the Uinta Subprovince and appears to bisect the two forks at the subprovince's western margin.

Economics

Along a trend defined by the general orientation of the crest of the Uinta Mountains is a much-studied, strongly mineralized belt, known by various names; such as the Uinta-Gold Hill Arch of Roberts (1960), the Oquirrh-Uinta Belt of Hilpert and Roberts (1969), and the Uinta-Gold Hill trend of Erickson (1976). A mineralized zone containing ten mining districts of variable importance is located within this belt along the Uinta Megalineament (figs. 5, 11) and is associated with this megalineament's intersection with the Wasatch East and Uncompahgre-Raft River Megalineaments.

TOWANTA MEGALINEAMENT

Description

The Towanta Megalineament (fig. 5) is traced for 89 km across the study area with an average trend of 70°. According to Ritzma (1976), the complete megalineament extends from an area 32 km north of Vernal, Utah, southwest to the vicinity of the House Range in western Utah. Ritzma maintains that the megalineament bends to the south where it crosses the Wasatch line. Close examination of the ERTS imagery (fig. 3) clearly demonstrates this "bending" to be only apparent. A packet of lineaments striking generally 40° cross and, for 14 km interrupt the trend of the Towanta Megalineament. Across this packet of lineaments the Towanta Megalineament is offset to the south, but continues to follow essentially the initial trend to Utah Valley where the megalineament disappears in the cultivated valley floor. For a detailed description of the entire trace of the Towanta Megalineament, see Ritzma (1976).

Structure

According to the latest available geologic map of the study area (Hintze unpublished), faulting and folding (fig. 7) are not major controls of the megalineament; however, alignment of streams and ridges along the trace is obvious.

Geophysics

The Towanta Megalineament closely follows an aeromagnetic trend (fig. 8) noted by Zietz and others (1969, 1976) and was postulated by them to be a regional belt of en echelon shear zones. The Towanta Megalineament is also aligned with an elongated negative gravity anomaly (Cook and others 1975; fig. 9) which trends westward to the eastern margin of Utah Valley, where it apparently ends abutting a gravity high. An accumulation of seismic events illustrated by Arabasz and others (1979) marks the eastward terminus of the Towanta Megalineament as it is displayed in the study area (fig. 10). The balance of the megalineament in the study area parallels a distinct line of seismic events located 10 km to the north. Basement (fig. 7) appears to exert a major control on the portion of the Towanta Megalineament in the study area. The southern margin of the Uinta Subprovince (fig. 7) matches remarkably well the trace of the Towanta Megalineament (Condie 1969).

Economics

Four relatively unimportant mining districts in the study area (Bullock 1962) are associated with the Towanta Megalineament (figs. 5, 11). The mining districts' location along or nearby the megalineament and their association with areas of this megalineament's intersection with three other megalineaments (Wasatch East, Wasatch West, and Badlands Cliffs) is notable (fig. 5).

Ritzma (1976) indicates a belief that the Towanta Megalineament controls the northern extent of the Alta-

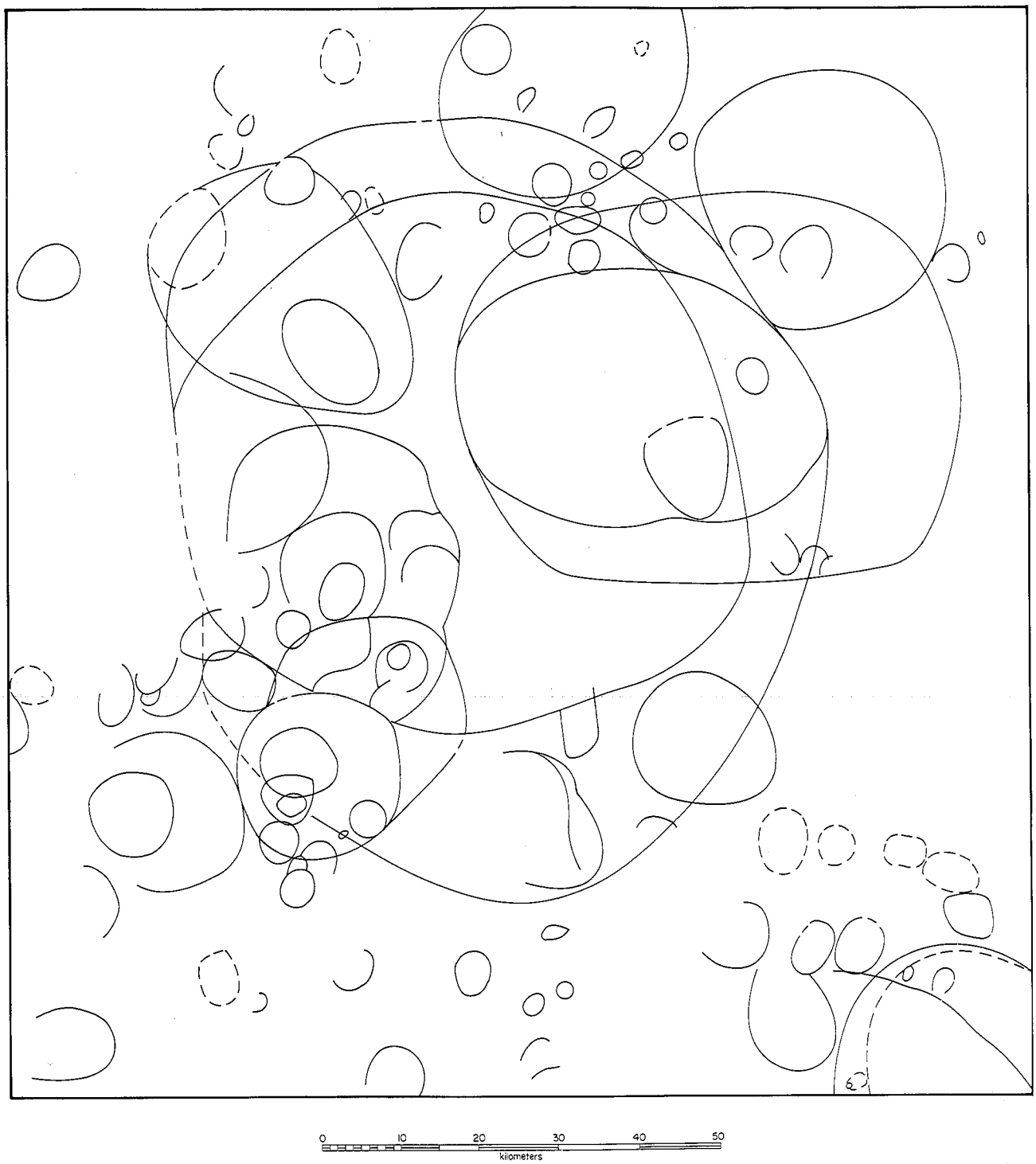

FIGURE 6.—*Annular structure map.*

mont-Bluebell oil field. An oil seep at Daniels Canyon and a zone of petroleum-saturated rock at Tabiona (fig. 11) are also associated with this megalineament.

A potential geothermal area in the Uinta Basin is plotted by the Utah Geological and Mineral Survey on their Energy Resources Map of Utah (map 44). It is likely that this megalineament is also a controlling factor in defining the northwest extent of the geothermal zone (figs. 5, 11).

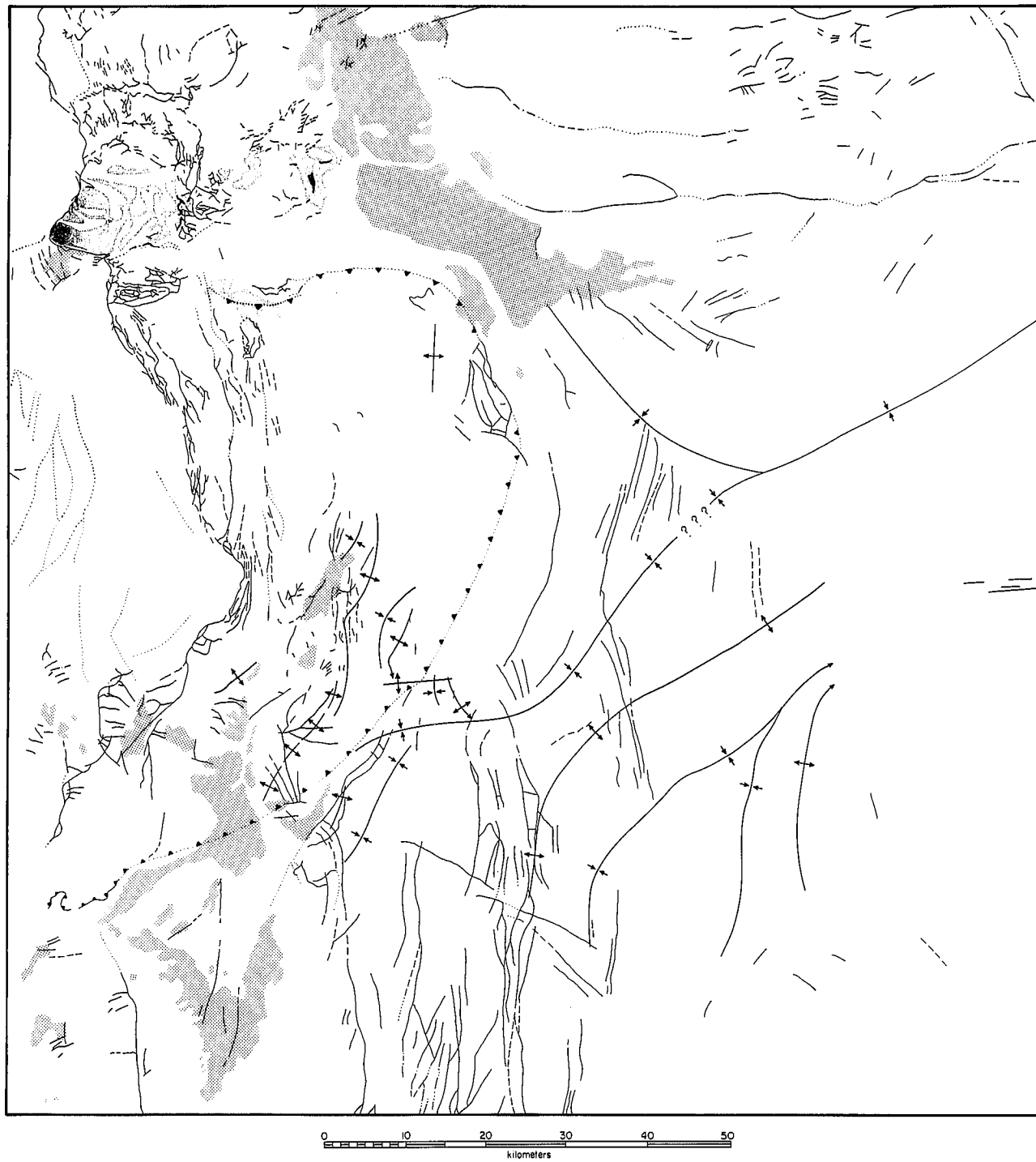

FIGURE 7.—*Tectonic map of study area. Data from Baker 1964a, 1964b, 1972, 1973, 1976; Baker and Crittenden 1961; Baker and others 1966; Bissell 1952; Bromfield and others 1970; Crittenden 1965a, 1965b, 1965c; Crittenden and others 1966; Hintze 1980; and Ritzma 1969.*

STRAWBERRY MEGALINEAMENT

Description

The east-west-trending Strawberry Megalineament extends for 135 km across northeastern Utah and is divided into two parts separated by the Scofield Megalineament (fig. 5). The eastern part of the Strawberry Megalineament is 76 km long, with its eastern terminus located 3 km south of Bridgeland, Utah, in the vicinity of Antelope Creek. It has an 89° trend and extends for 62 km from the eastern boundary of the study area to Strawberry Valley, where the megalineament is obscured for 12 km and sub-

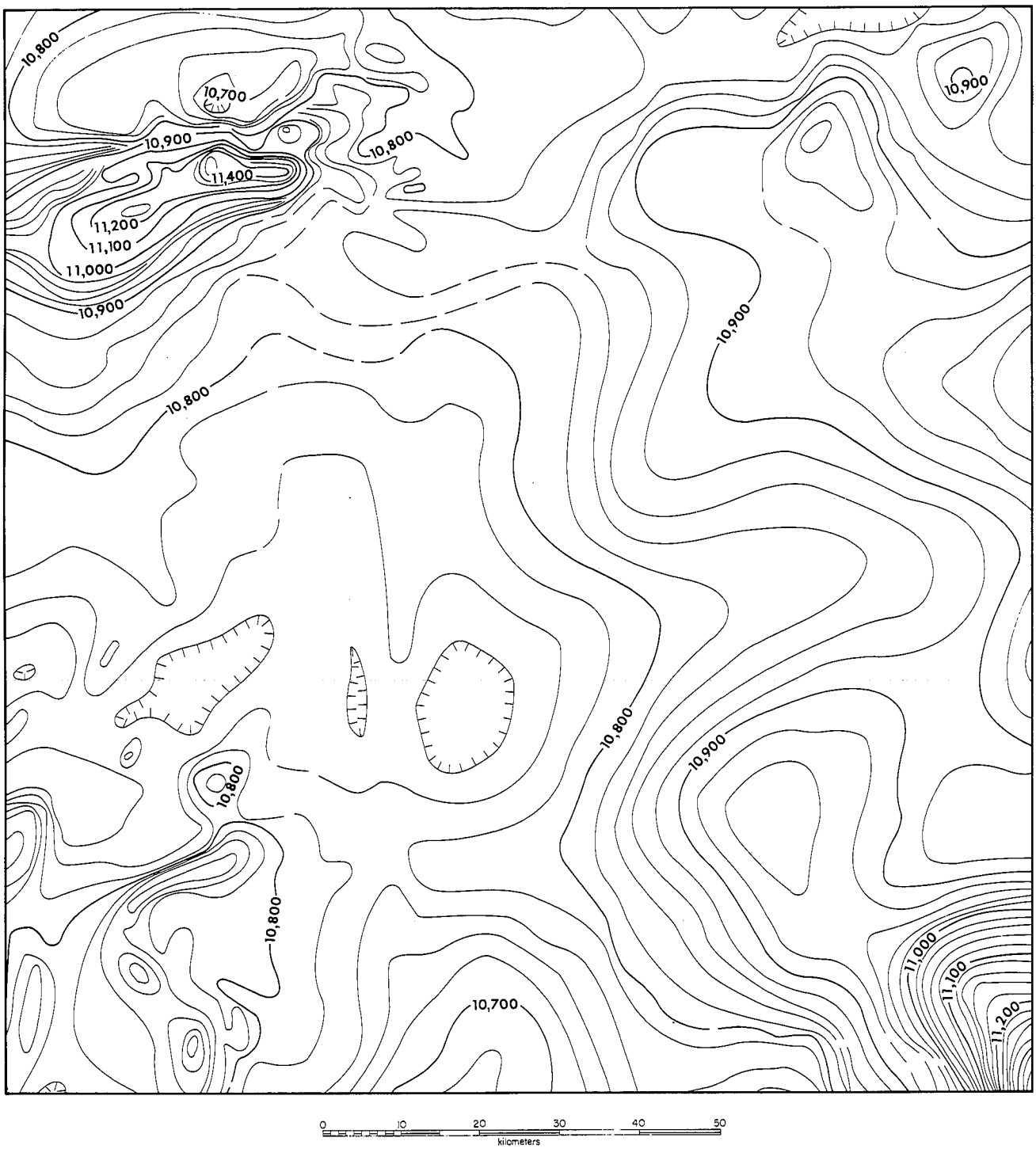

FIGURE 8.—*Aeromagnetic map (data from Zietz 1976).*

sequently offset to the south approximately 5 km. The trace then resumes but with a curvilinear conformation which, for convenience, has been drafted on the composite linear map (fig. 4) as two intercepting lineations. This variable trend, which curves to the southwest, characterizes this portion of the megalineament, which has a length of 59 km, with the western terminus located in the Wasatch Mountains 11 km south of Payson, Utah.

The megalineament is expressed as a linear albedo pattern corresponding to the Duchesne fault zone and converges westward with the essentially linear Strawberry River Valley. The previously mentioned interruption of this part of the megalineament occurs at the fault line scarp of the Strawberry Reservoir fault (figs. 5, 7). The

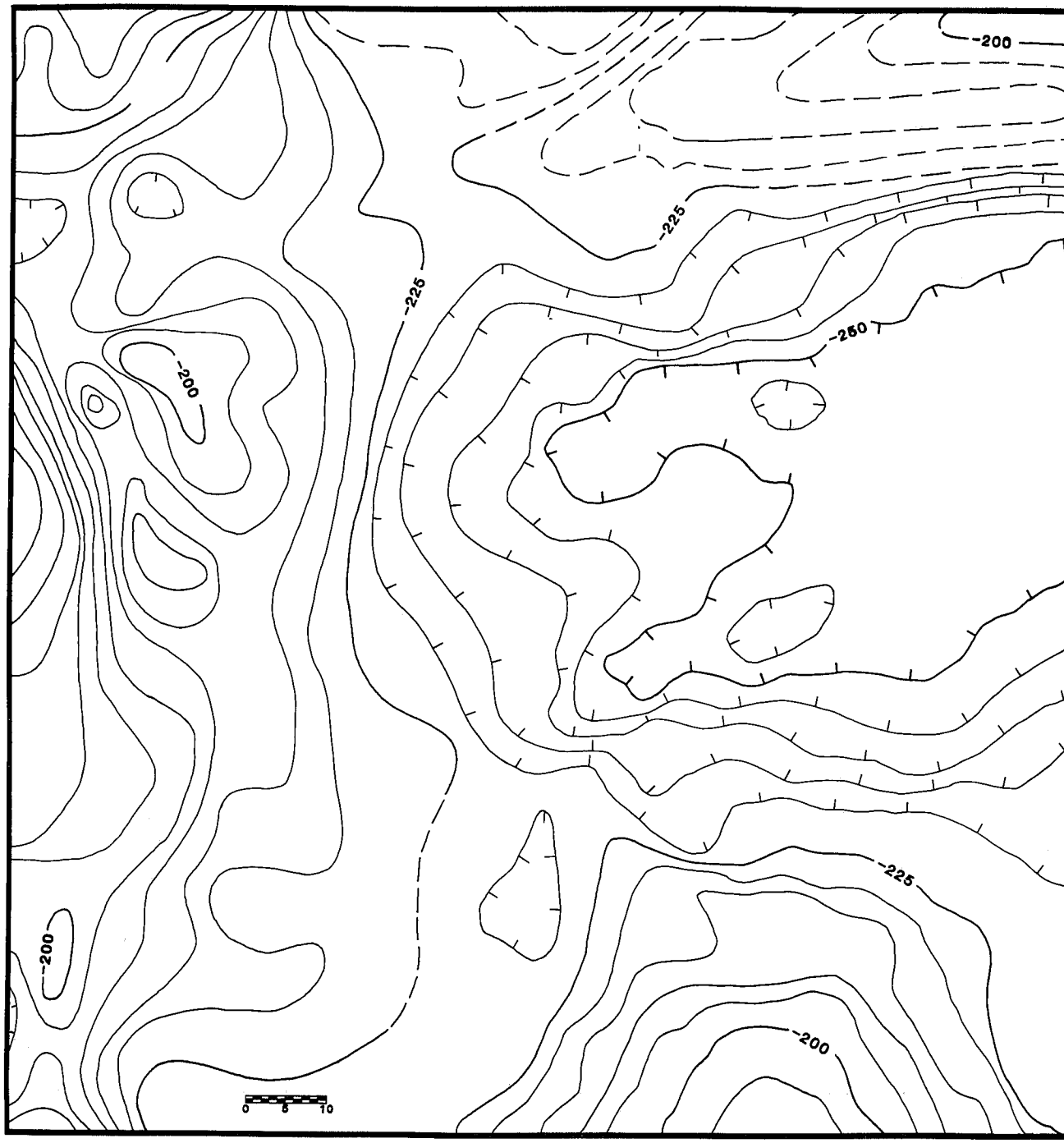

FIGURE 9.—*Bouguer gravity map of study area (Data from Cook and others 1975).*

offset western portion of the megalineament is expressed as the arcuate valley of Diamond Fork Creek which converges with a southwest-trending ridge on Loafer Mountain marking the gradual western termination of the megalineament in the study area.

Structure

The eastern section of the Strawberry Megalineament corresponds exactly with the Duchesne fault zone (figs. 5, 7). No other folding or faulting is associated with this megalineament.

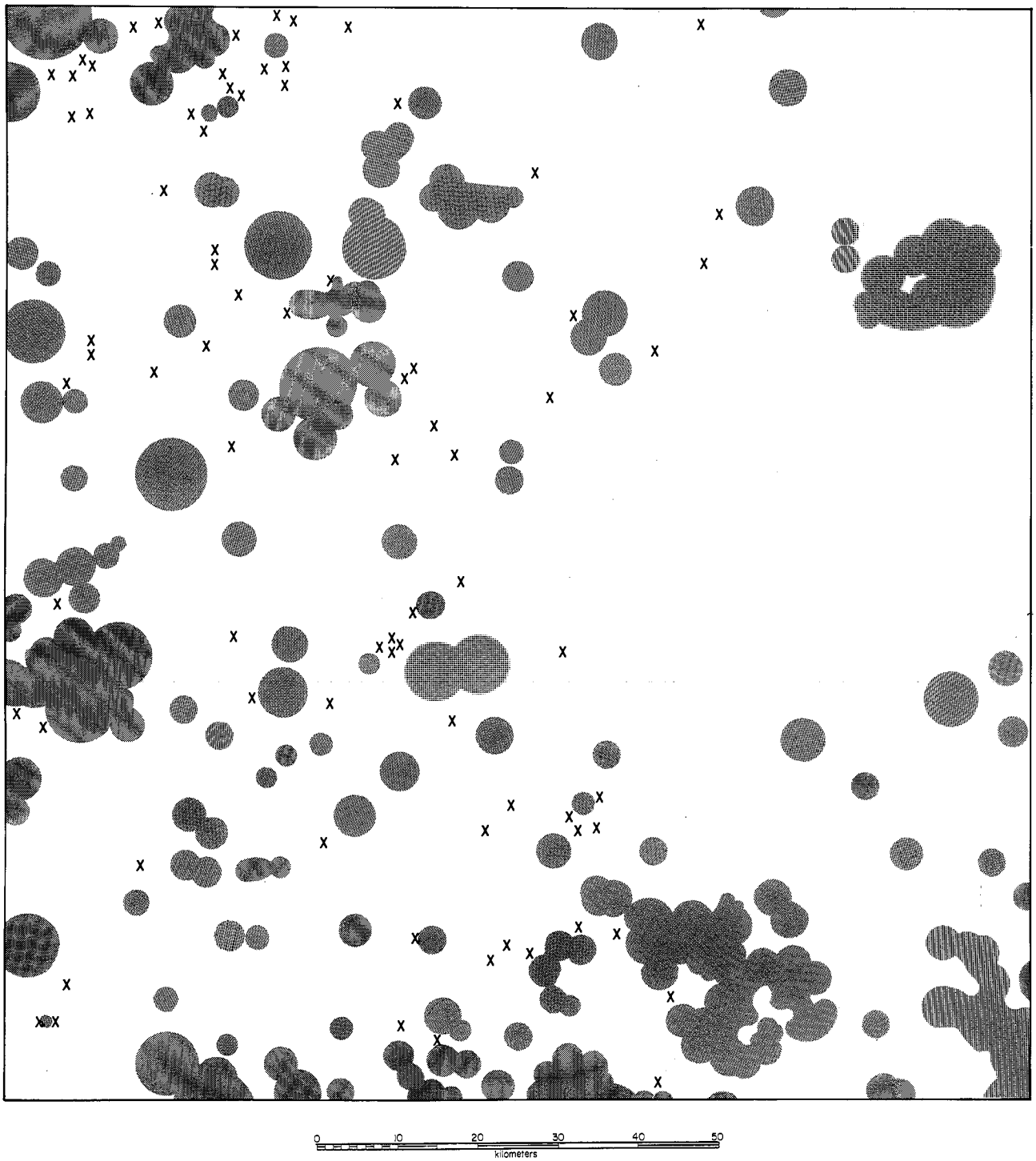

FIGURE 10.—*Schematic epicenter plot of the study area (after Arabasz and others 1979).*

Geophysics

The eastern part of the 89° trending Strawberry Megalineament is associated with, but subparallel to, an aeromagnetic trough (Zietz 1976; fig. 8) trending 77° with the western curvilinear portion of the megalineament correlating with an elongate aeromagnetic minimum possessing a 57° trend. A gravity trend for the eastern portion of the Strawberry Megalineament mirrors the 77° aeromagnetic trend (Cook and others 1975; fig. 9); however, the western curvilinear portion is not associated with a

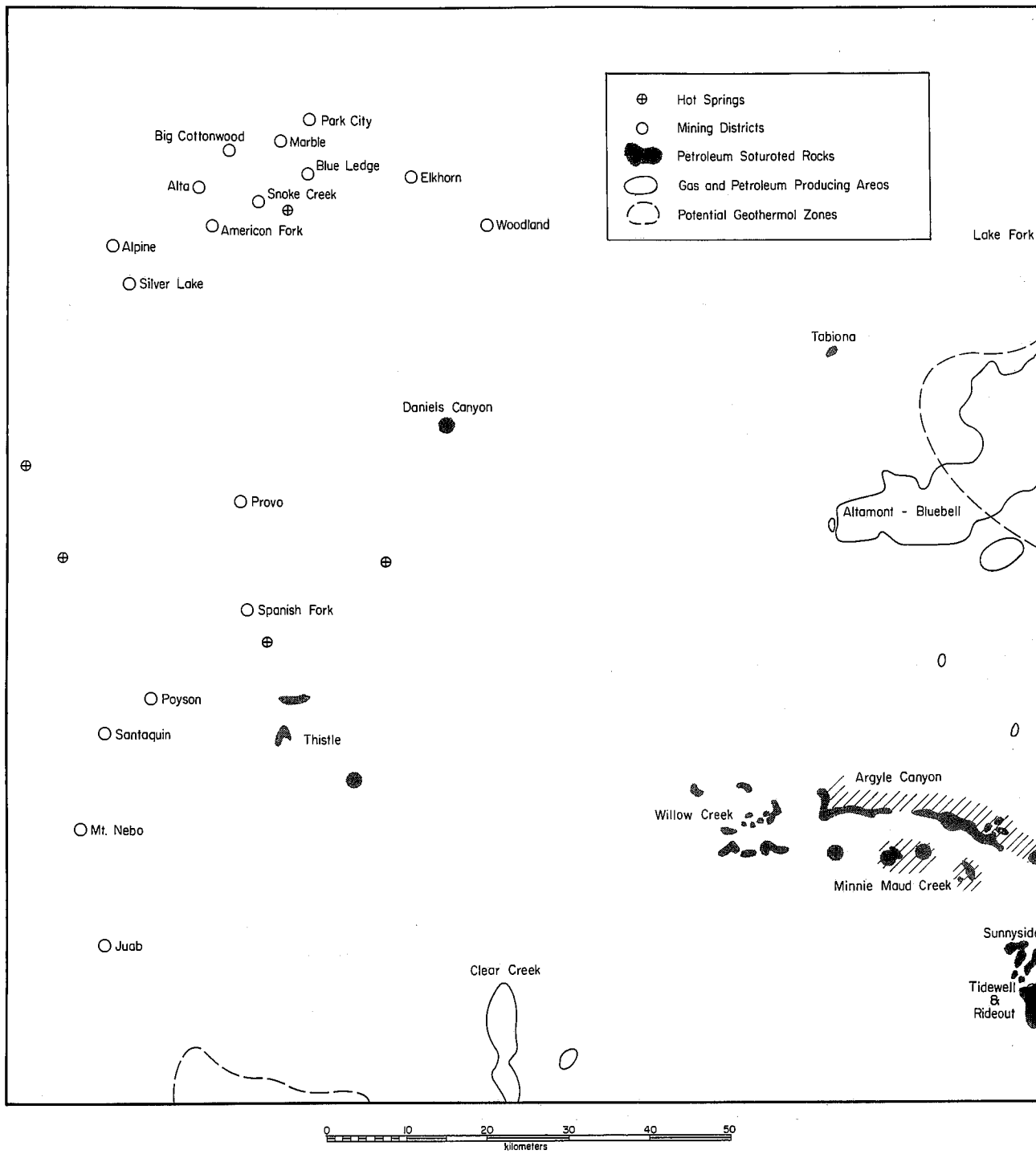

FIGURE 11.—*Economic geology map of the study area. Data from Utah Geologic and Mineral Survey Map 44, Energy Resources Map, Utah 1977.*

linear gravity trend. The curvilinear portion is, however, associated, at their mutual intersection, with an abrupt constriction of a north-south gravity ridge. There is no evidence for seismic control of the eastern portion of the Strawberry Megalineament. Indeed, no record of seismic activity in the area is plotted at all (fig. 10; Arabasz and others 1979). Although it is too sparse to define a pattern of control, scattered seismic activity is plotted in the vicinity of the curvilinear part of the megalineament. No basement control is indicated for the eastern section of the Strawberry Megalineament. However, the zone of greatest flexure of the curvilinear western portion of the megalineament correlates well with the Big Cottonwood Subprovince boundary (fig. 6), probably reflecting some basement influence (Condie 1969).

Economics

The curvilinear western portion of the megalineament is associated with and is a credible controlling factor in the localization of the Mt. Nebo mining district (fig. 11).

The southwest margin of the Altamont-Bluebell oil field (fig. 11) lies parallel to and 4 km north of this megalineament. It appears likely that the Strawberry Megalineament is at least a controlling factor in the positioning of this field. The southern extent of the previously mentioned potential geothermal field in the Uinta Basin (fig. 11) also appears to be at least partially controlled by this megalineament.

BADLANDS CLIFFS AND BOOK CLIFFS MEGALINEAMENTS

A brief explanation concerning the treatment of the Badlands Cliffs and Book Cliffs Megalineaments is in order. Within the study area, the two are parallel with approximately 19 km separation and could easily be considered a single broad linear zone. However, eastward, outside the study area, a divergence in trend and dissimilar length dictate the necessity of separate discussion.

Badlands Cliffs Megalineament

Description. The Badlands Cliffs Megalineament (fig. 5), which extends beyond both the east and west borders of the study area, is traced for 129 km across the study area displaying a 280° trend. Eastward, the megalineament is traced to the western margin of the Roan Plateau at Green River Canyon. Across the Roan Plateau, the trace is diminished and is marked solely by an alignment of drainage direction changes. After crossing the Roan Plateau, the megalineament, or a similar linear feature, resumes and is traced into central Colorado near Mount Lincoln. Westward of the study area, the megalineament is marked by an alignment of mountain ranges ending at the Dugway Range in western Utah.

The Badlands Cliffs Megalineament is initially expressed in the study area by the lip of the Badlands Cliffs. The trace is interrupted for 18 km by a large annular structure (fig. 6) imprinted in the Eocene surface rocks along the Badlands Cliffs. The megalineament resumes following Soldier Creek Canyon to Thistle Junction where the trace is defined by alignment of mountain ranges and albedo patterns in the Basin and Range Province. The trend appears to end at the Dugway Range but may continue westward masked by the great Salt Lake Desert.

Structure. No structural control of the megalineament by folding is evident because folding trends are essentially normal to the megalineament. Except in the western part of the study area, faulting trends are also normal to this megalineament (fig. 7). At Thistle Junction (fig. 1), fault trends begin to parallel, with little divergence, the megalineament, making fault control for it along this portion likely.

Geophysics. The Badlands Cliffs Megalineament corresponds with an aeromagnetic ridge (Zietz 1976; fig. 8) in the eastern part of the study area which gradually changes to a chain of aeromagnetic minimums in the west. A slight gravity trend (Cook and others 1975; fig. 9) is associated with the megalineament but is not as obviously correlative as the above described aeromagnetic trend. In the eastern part of the study area, the gravity trend is defined by the southern margin of the Uinta Basin gravity minimum. Westward, the gravity contours trend north-south, yet, where intersected by the megalineament, tend to deflect to an east-west trend. Beyond this zone of intersection, the gravity contours resume their original north-south trend. Seismic activity along the Badlands Cliffs Megalineament tends to cluster at intersections with other megalineaments (Arabasz and others 1979). Otherwise, recorded seismic activity along the megalineament is too meager and scattered to postulate a controlling mechanism.

Economics. This megalineament is associated with vast deposits of petroleum-saturated rocks (figs. 5, 11) located near the southeast corner of the study area. Westward from this point, the Badlands Cliffs Megalineament defines the northerly extent of these outcrops of petroleum-saturated rocks at Argyle Canyon and Willow Creek. Farther to the west, the deposits of petroleum-saturated rocks near Thistle are associated with this megalineament at its intersection with the Wasatch East Megalineament.

Book Cliffs Megalineament

Description. The Book Cliffs Megalineament (fig. 5), which extends for 129 km across the study area with a trend of 280°, is parallel to and 19 km south of the Bad-

lands Cliffs Megalineament. It extends beyond both the east and west borders of the study area. East of the study area, it is marked by an alignment of stream valleys across the Roan Plateau and the Book Cliffs of Colorado, where it veers to the south and ends near La Junta, Colorado, at a sharp northeastward bend of the Arkansas River. Westward from the study area, an apparent merging occurs with the Badlands Cliffs Megalineament with both megalineaments ending at the Dugway Range in western Utah.

The megalineament is initially expressed in the study area by the rim of the Book Cliffs (figs. 3, 5) west of Castlegate, Utah, where east-west topographic trends define its trace. East-west-trending valleys and ridges define the megalineament across the Wasatch Plateau and the Wasatch Range, which is crossed near the south end of Dry Mountain in Utah County.

Structure. With only two subparallel exceptions (fig. 7), folding and faulting trends are basically perpendicular to the Book Cliffs Megalineament; therefore, no structural control is postulated.

Geophysics. The Book Cliffs Megalineament correlates with an east-west aeromagnetic trend which is related to the aeromagnetic trend described in the Badlands Cliffs segment (Zietz 1976; fig. 8). The megalineament also correlates with a rather obscure gravity trend (Cook and others 1975; fig. 9) initially associated with the northern end of the San Rafael Swell gravity high, then goes westward, with an east-west bulge in the Scofield Reservoir gravity minimum and with contour-line deflections across the Wasatch Range. A well-defined linear seismic pattern (Arabasz and others 1979; fig. 10) in the eastern portion of the study area which diminishes westward owing to scattering of the seismic pattern is associated with the Book Cliffs Megalineament.

Economics. The Mt. Nebo mining district (fig. 11) lies on the Book Cliffs Megalineament near its intersection with the Wasatch West and Strawberry Megalineaments (fig. 5). Coal is mined near Sunnyside, Utah (fig. 11), along this megalineament.

Also, near Sunnyside, Utah (fig. 11), the previously mentioned deposits of petroleum-saturated rock are exposed, trending essentially east-west and located between the Badlands Cliffs and Book Cliffs Megalineaments (figs. 5, 11). The Book Cliffs Megalineament controls the southern extent of these deposits in the study area.

UNCOMPAHGRE-RAFT RIVER MEGALINEAMENT

Description

The Uncompahgre-Raft River Megalineament (fig. 5) is the largest linear feature observed in the study area and extends beyond the borders of the study area, both to the northwest and to the southeast. Although the trace of the megalineament is not strictly continuous for its entire length, examination of tectonic maps (King 1969, 1977), a satellite imagery conterminous mosaic of the United States (NASA 1974), a landform map of the United States (Raisz 1957), raised relief maps of the United States and North America (Nystrom maps NR1 and NR2), and a survey of literature (Raisz 1945, Kelley 1955, Heylmun 1959, Moody 1966, Stone 1974, and Warner 1980) indicate a megalineament of great length. These data are good indications for the extension of the Uncompahgre-Raft River Megalineament from the Isthmus of Tehuantepec in southern Mexico to Queen Charlotte Island off the British Columbia coast. Interruptions and possible offsets of this megalineament may be of great tectonic and economic importance.

In the study area, the Uncompahgre-Raft River Megalineament extends for 172 km with a 318° trend (fig. 5) from near Sunnyside, Utah, in the southeast, to the Salt Lake Salient in the northwest. In the study area, near Sunnyside, Utah, initial expression of the megalineament is by alignment of ridges and valleys which to the northwest is interrupted by a large annular structure (fig. 6) developed at the intersection of this megalineament and the Badlands Cliffs Megalineament. Resuming northwestward, the megalineament is marked by the northwest-trending northern margin of Strawberry Valley. Alignment of ridges and valleys resume the outline of the megalineament and continue to the Salt Lake Salient.

Structure

Faulting (fig. 7), with one exception, exerts no control on the megalineament. Northwest of Strawberry Reservoir (fig. 1), faulting, exposed in a window through the Charleston thrust plate, correlates with and somewhat parallels the Uncompahgre-Raft River Megalineament. The exposed window is located in the intersection zone (fig. 5) of the Towanta, Scofield, and Uncompahgre-Raft River Megalineaments. Indeed, this window, because of possibly more pervasive fracturing of the rocks in the intersection zone, may be a response of differential erosion. Folding trends (fig. 7) are essentially normal to the megalineament.

Geophysics

A distinct northwestward aeromagnetic trend (Zietz and others 1976; fig. 8) consisting of a linear chain of magnetic highs, coincides with the Uncompahgre-Raft River Megalineament. No discernible gravity trend (Cook and others 1975; fig. 9), however, is associated with it. In the southeast portion of the study area, there is excellent evidence correlating seismic activity (Arabasz and others

1979; fig. 10) and the Uncompahgre-Raft River Megalineament; however, north of the Badlands Cliffs Megalineament (fig. 5), within the Uinta Basin, seismic activity virtually ceases. Northwest of Strawberry Reservoir (fig. 1), seismic activity resumes, but recorded epicenters are very scattered and little linear trend is recognized, so seismic control of this portion of the megalineament is not postulated.

Economics

Major ore mineralization (fig. 11), mentioned earlier, within the zone of intersection of the Uncompahgre-Raft River, Wasatch East, and Uinta Megalineaments (fig. 5) and coal mining near Sunnyside, Utah (fig. 11), comprise the mining districts associated with this megalineament.

Petroleum associations with this megalineament include the petroleum-saturated rock deposits near the southeast corner of the study area (fig. 11) which are related to the intersection of this megalineament with the Badlands Cliffs and the Book Cliffs Megalineaments and the previously mentioned oil seep at Daniels Canyon (fig. 11).

SCOFIELD MEGALINEAMENT

Description

The Scofield Megalineament (fig. 5) extends for 136 km through the study area with a trend of 356°. The megalineament, with a total length of 169 km, extends beyond both the southern and northern borders of the study area, with its southern terminus located in Huntington Creek Canyon 13 km northwest of Huntington, Utah. Geomorphic expression of the megalineament is defined by north-south-trending valleys and ridges. Near Kamas, Utah, expression of the megalineament begins to wane, but it is distinguishable to its northern end 10 km east of Coalville, Utah.

Structure

Fault control of the Scofield Megalineament south of its intersection with the Strawberry Megalineament is obvious (fig. 7). However, with one exception, north of the Strawberry Megalineament intersection, faulting is not a controlling factor. Here, faulting trends are parallel to subparallel to the megalineament, but they are located far to the west. In the zone where the Scofield, Towanta, and Uncompahgre-Raft River Megalineaments intersect (fig. 5), faulting, exposed in a window through the Charleston thrust plate, is associated for a short distance with the trace of the Scofield Megalineament. Inasmuch as folding trends are oblique to the megalineament, folding is not considered a controlling structural factor.

Geophysics

A weakly developed aeromagnetic trend (Zietz and others 1976; fig. 8), extending from an aeromagnetic high on the southern border of the study area to a site 25 km north of Strawberry Reservoir, marks the trace of the Scofield Megalineament. In this vicinity, a southwest aeromagnetic trend associated with the South Flank fault of the Uinta Mountains and the previously described aeromagnetic trend associated with the Towanta Megalineament interact with the north-south Scofield aeromagnetic trend resulting in its obfuscation and termination. South of Strawberry Reservoir, a weak gravity trend (Cook and others 1975; fig. 9) is defined by an elongate gravity minimum positioned around Scofield Reservoir. This gravity trend continues northward marked by east-west-trending gravity contours bending suddenly northward to the Scofield Megalineament. North of the Scofield-Strawberry Megalineament intersection, the trend abruptly ends. A number of seismic events (Arabasz and others 1979; fig. 10) are on or near the Scofield Megalineament but are too scattered to portend seismic control.

Economics

The Elkhorn and Woodland mining districts (fig. 11) are associated with this megalineament (fig. 5) near its intersection with the Uinta Megalineament.

The Clear Creek gas field (fig. 11) is flawlessly aligned with the Scofield Megalineament. The previously mentioned oil seep at Daniels Canyon (fig. 11) is also located on this megalineament near its intersection with the Towanta and Uncompahgre-Raft River Megalineaments.

WASATCH EAST MEGALINEAMENT

Description

The Wasatch East Megalineament (fig. 5) is traced for 149 km across the study area with a trend of 347° and, like the others previously described, is followed beyond the borders of the study area. To the north, the trace is followed to the Snake River Plain near Pocatello, Idaho, and south of the study area, extends to the southern end of East Mountain, northeast of Castledale, Utah, measuring a total length of 420 km. Initial expression of the megalineament in the study area, from north to south, is by the crest of the central Wasatch Mountains. South of Provo Canyon, the central Wasatch Range widens abruptly, where the Wasatch East Megalineament intersects both the Towanta and Strawberry Megalineaments. A large ellipsoidal annular structure (fig. 6), defining the abrupt widening of the central Wasatch Range, results and is characterized by a number of smaller annular structures contained within itself. The axis of this large annular

structure maintains the trend of the Wasatch East Megalineament. Within the confines of this annular structure, expression of the Wasatch East Megalineament is transformed from the crest of the central Wasatch Mountains to the broader yet continuous linear trending Wasatch Plateau (fig. 2). A complex series of megalineament interactions is displayed in and near the area of the above mentioned annular structure which is illustrated by the following: (1) within a relatively small area, the Towanta Megalineament intersects the Wasatch East Megalineament and is offset left laterally to the south; (2) the curvilinear portion of the Strawberry Megalineament intersects the Wasatch East, Badlands Cliffs, Wasatch West, and Book Cliffs Megalineaments with no discernible offset; (3) the Wasatch East Megalineament intersects the Towanta, curvilinear portion of the Strawberry, the Badlands Cliffs, and the Book Cliffs Megalineaments with a continuance of trend.

Structure

North of Provo Canyon, the megalineament is constantly defined by or closely paralleled by faulting (fig. 7); however, south of Provo Canyon, within the annular structure previously mentioned, this faulting diminishes gradually. Beyond the zone of intersection with the Towanta Megalineament, near Hobble Creek Canyon, faulting trends are seldom parallel and are usually oblique to the trend of the Wasatch East Megalineament. After the Wasatch East Megalineament's transition to the Wasatch Plateau (fig. 2), parallel faulting again is intimately involved with the megalineament, and folding is oblique.

Geophysics

A well-defined aeromagnetic trend (Zietz and others 1976; fig. 8), which lies approximately 7 km to the east and parallels the Wasatch East Megalineament, consists of a south-trending aeromagnetic trough descending from the magnetic high associated with the Little Cottonwood Stock (fig. 6). A less well defined gravity trend (Cook and others, 1975; fig. 9) is observed which consists of aligned gravity minimums in the north deteriorating to a linear gravity slope paralleling the megalineament in the south. Recorded seismic events (Arabasz and others 1979; fig. 10) are scattered along the trace of the Wasatch East Megalineament, but while seismic episode frequency increases, and the pattern tightens south of the Towanta Megalineament intersection (fig. 5), the evidence is inconclusive for seismic control.

Economics

The Provo and Spanish Fork mining districts (fig. 11) are associated with this megalineament. The Provo district is related to the intersection of this megalineament and the northerly offset portion of the Towanta Megalineament (fig. 5), while the Spanish Fork district is associated with the Wasatch East Megalineament and the southerly offset portion of the Towanta Megalineament.

Petroleum association along this megalineament is involved only with the petroleum-saturated rocks of the Thistle area (fig. 11).

A hot spring (fig. 11) is located very near the trace of the megalineament just north of its intersection with the Badlands Cliffs Megalineament.

WASATCH WEST MEGALINEAMENT

Description

The Wasatch West Megalineament (fig. 5) extends for 55 km across the study area with a trend of 3° and extends southward beyond the borders of the study area, terminating at the southern end of the San Pitch Mountains east of Gunnison, Utah. The megalineament has a total length of 94 km. This is 6 km less than the stated minimum megalineament length, but, because I consider it to be genetically related to the Wasatch East Megalineament and because it is just short of the defined criterion, I have chosen to include the Wasatch West Megalineament with the megalineaments. It is expressed as the north-south-trending crest of the southern Wasatch Mountains and the San Pitch Mountains.

Structure

Faulting (fig. 7) plays a determinant role in the northern portion of the megalineament; however, south of the intersection with the curvilinear portion of the Strawberry Megalineament (fig. 5), northeast of Mona, Utah, faulting trends are not associated with the megalineament. Folding (fig. 7) appears to play little or no part in the trace of the megalineament.

Geophysics

Aeromagnetic trends (Zietz and others 1976; fig. 8) do not appear to be associated with this megalineament because they trend southwest to northeast, oblique to the nearly north-south trace of the megalineament. A small north-south-trending gravity high (Cook and others 1975; fig. 9) parallels the megalineament 5 km to the west. Otherwise, the megalineament parallels a north-south-trending gravity slope. Although seismic activity (Arabasz and others 1979; fig. 10) is intense near the northern terminus of the Wasatch West Megalineament at its intersection with the Badlands Cliffs and the Towanta Megalineaments, evidence for seismic control along the length of the megalineament is lacking.

Economics

The Juab and Santaquin mining districts (fig. 11) are located along this megalineament. The Mount Nebo mining district is within the intersection zone of this megalineament and the Strawberry and Book Cliffs Megalineaments (figs. 5, 11).

This megalineament may be a control for the western margin of a potential geothermal area mapped by the Utah Geological and Mineral Survey (fig. 11) plotted on their "Energy Resources of Utah," map 44.

ANALYSIS

GENERAL STATEMENT

Measurement and subsequent plotting of 651 linear trends indicate preferred directions of linear occurrence. Eight linear sets (fig. 12) exhibiting varying degrees of development are recognized. Each set is related to a mutually orthogonal set, forming a pairset (Gay 1973) and a tetraorthogonal pattern results (fig. 12).

Linear Pairset	*Trend*	*Angular Separation*
A–A′	260°–350°	90°
B–B′	373°–0°	87°
C–C′	289°–15°	87°
D–D′	337°–73°	95°

Five of these eight linear trends correspond favorably with linear trends recognized by Gay (1972) in the Paradox Basin, Utah, 350 km southeast of this study area. The two principle orthogonal pairsets in this study area, C–C′ and D–D′, are similar to the Uncompahgre (298°)-Wasatch (22°) and the Front Range (338°)-Uinta (69°) pairsets of Gay (1972).

Young	*Gay*		*Angular Separation*
C 289°	Uncompahgre	298°	9°
C′ 15°	Wasatch	22°	7°
D 337°	Front Range	338°	1°
D′ 73°	Uinta	69°	4°

This striking correlation of widely separated independent studies documents favorable evidence for regional control of major linear trends in the Colorado Plateau and the Uinta-Wasatch transition zone.

COMPUTER ANALYSIS

Analysis of linear intersection frequency and linear density was initiated by preparing a grid overlay with 20 mm × 20 mm cells (7 km map scale). The unit cell size was chosen merely for convenience. The resulting grid overlay was placed over the linear map (fig. 4), and the number of linear intersections per unit cell was recorded. Measurement of total linear length per unit cell (linear density) was also recorded. The data derived for intersection frequency and linear density were inserted separately into the SYMAP program and processed through the IBM 360 computer. Two machine-generated contour maps (fig. 13, 14) illustrating, respectively, linear intersection frequency and linear density completed the procedure.

Linear Intersection Frequency

Examination of the linear intersection frequency contour map (fig. 13) reveals a number of anomalies, the majority of which occur in the southern half of the study area. All the larger anomalies occur there. Correlation of medium- to high-amplitude anomalies with zones of megalineament intersection (figs. 5, 13) is obvious. Mineralization (fig. 11) correlates strikingly with areas of low-to medium-amplitude anomalies (fig. 13) in the northwestern quadrant of the study area and in a belt near the study area's western margin. The reader's attention is especially directed to the Big Cottonwood, Spanish Fork, and Mt. Nebo mining districts (figs. 5, 11).

With one major exception, petroleum and natural gas occurrence and petroleum-saturated rock outcrops (fig. 11) are conspicuously associated with medium- to high-amplitude linear intersection frequency anomalies (fig.

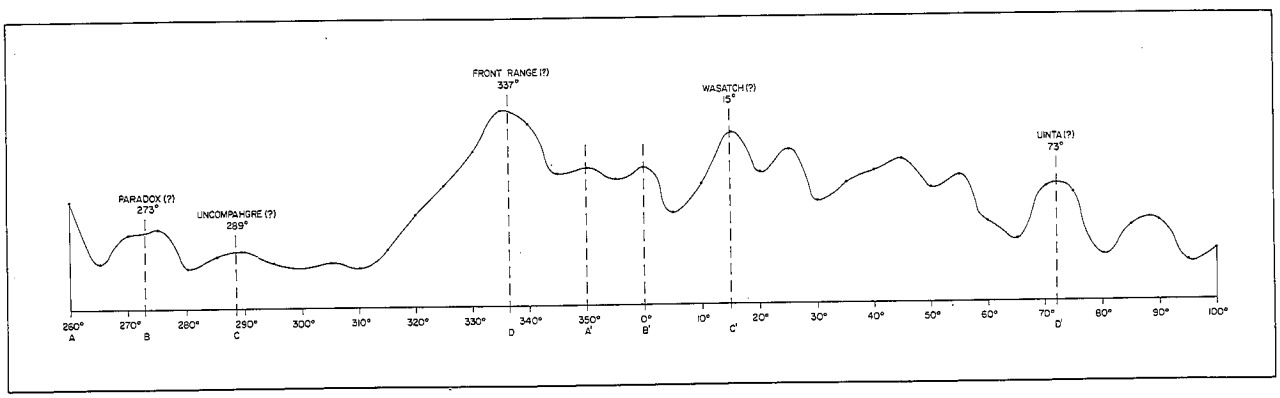

FIGURE 12.—*Orientation histogram of preferred linear directions in the study area compared with data from Gay 1972.*

13) located in the southern half of the study area. Particular attention is directed to the Thistle area, to the Clear Creek gas field area, and to a belt of northwest-trending anomalies beginning near Sunnyside, Utah (fig. 11), which define, in large measure, the vast expanse of petroleum-saturated rock outcrops in the area. The major exception noted above, wherein no correlation is recognized, is the Altamont-Bluebell oil field. Examination of ERTS image

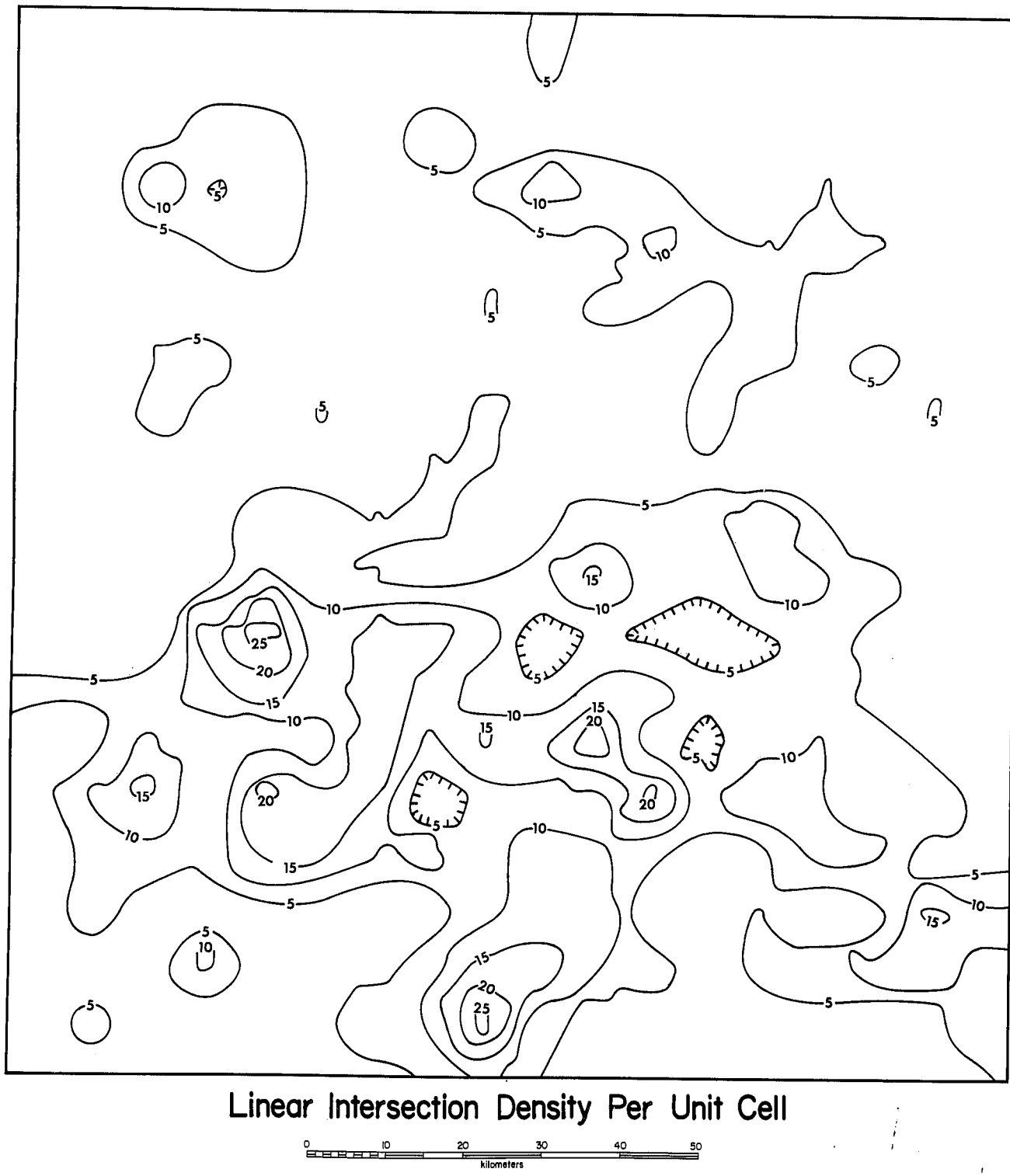

FIGURE 13.—*Linear intersection frequency per unit cell contour map.*

5544-16413 (fig. 3) reveals a substantial number of small linears, less than 4 km in length, located in the area of the Altamont-Bluebell oil field. Had the discrimination level of 4 km linear length not filtered out the smaller linears, a better correlation may have resulted. It poses an interesting project to be developed in another study.

Two hot springs are associated with linear intersection frequency anomalies (Young 1976). A hot spring located near the center of T. 3 S, R. 4 E, is located within a low-amplitude anomaly 8 km north of Deer Creek Reservoir (fig. 11). Another hot spring located in the northwest quarter of T. 9 S, R. 4 E, is directly centered in one of the two highest-amplitude anomalies mapped. Three other hot springs are not associated with anomalies. Two are located in Utah Valley near Utah Lake (fig. 11), where detection of linears is difficult if not impossible because cultural features mask or otherwise disguise the linear traces.

Linear Density

Linear density (the number of kilometers of linear per unit cell) correlates favorably with the linear intersection frequency contour map. However, finer detail and perhaps more information is available by contouring linear density. Anomalous highs equate with linear intersection frequency highs, varying only in shape. Information presented above relating linear intersection frequency data to areas of economic interest apply equally well to linear density data with the following added information. The 14- and 21-km density contours in the east central portion of the study area outline the Altamont-Bluebell oil field (fig. 11, 14). Although the area defined is somewhat larger than the area of the Altamont-Bluebell field outlined in map 44 of the Utah Geological and Mineral Survey's "Energy Resources Map of Utah," the shape is reproduced with remarkable persistence. In view of these data, linear density analysis, at least in this area, may be less affected by the filtering effect of linear length selection. Two anomalously low areas are, however, present within the outline of the Altamont-Bluebell oil field (fig. 14). These anomalous low areas may also be due to the filtering effect. Twenty other anomalously low areas occur in the study area. No other explanation is proposed at this time.

ANNULAR STRUCTURES

GENERAL STATEMENT

One hundred sixteen annular structures (fig. 6) are identified in the study area and range in size from a long axis diameter of 100 km to less than 1 km, with shapes varying from nearly circular to roughly ellipsoidal (Glukhovskiy 1977). Other curved features are noted (curvilinears, Peterson 1976, Smith 1976), but unless 75 percent closure of the ring is displayed, they are not included in this study. Annular structures are expressed by ridges and valleys with arcuate trends (compare fig. 3 and fig. 6), arcuate drainage patterns, and arcuate tonal anomalies, which are often the only expression of smaller annular structures.

The long axes of ellipsoidal annular structures generally follow the trend of an associated megalineament (compare fig. 3 and fig. 5) and, with one exception, are associated with megalineament intersections. The exception, a 34-km-diameter annular structure located at the northeastern terminus of the Towanta Megalineament (fig. 5), is centered around and evidently associated with the intersection of two large (approximately 40-km length) lineaments (fig. 4). Two large (100-km and 75-km diameter) concentric annular structures dominate the central part of the study area and form the transition zone between the Uinta Mountains, Wasatch Mountains, and Colorado Plateau. Thirteen megalineament intersections occur within or near the borders of these large annular structures. Centered within them and very likely playing a major role in their genesis is the zone of intersection of the Uncompahgre-Raft River, Scofield, and Towanta Megalineaments. Within the interiors and along the borders of these two large annular structures are a number of smaller ones; the majority of which are closely associated with megalineaments and megalineament intersections. The consistent association of annular structures and megalineament intersection suggests intimate relationship.

SUMMARY

Lineations are present throughout the study area and are obscured only in those areas where lakes, cultivation, and cultural features mask their presence (fig. 4). They are characterized by remarkably straight trends, and the majority are the undoubted result of complex and, at present, enigmatic interactions within the lithosphere. While lineation patterns are regionally ordered and systematic (fig. 4, 12), within this regional order more locally restricted stress fields may be recognized. The display of four separate lineation patterns separated by megalineaments, which have supporting aeromagnetic and gravity data, suggests four discrete basement blocks whose common margins are displayed at the surface as large-scale rectilinear features (megalineaments) (Affleck 1963).

Correlation of mineralized districts, areas of petroleum and natural gas accumulation, and hot spring occurrence with lineation intersection frequency (fig. 13) and lineation density anomalies (fig. 14) is notable and suggests careful examination of other anomalous areas not now known to have economic value. Lineation-density and intersection-frequency anomalies are probably associated with zones of intense fracturing in the subsurface, generating zones of weakness facilitating magmatic intrusion

and hydrothermal fluid dispersion in mineralized districts or creating fracture permeability for avenues of migration and/or zones of accumulation of hydrocarbons.

Mining districts lie on or near megalineaments, and megalineament intersections appear to be a significant factor in ore emplacement (fig. 11). Outcrops of petroleum-saturated rock and areas of natural gas production are also associated with megalineaments and their inter-

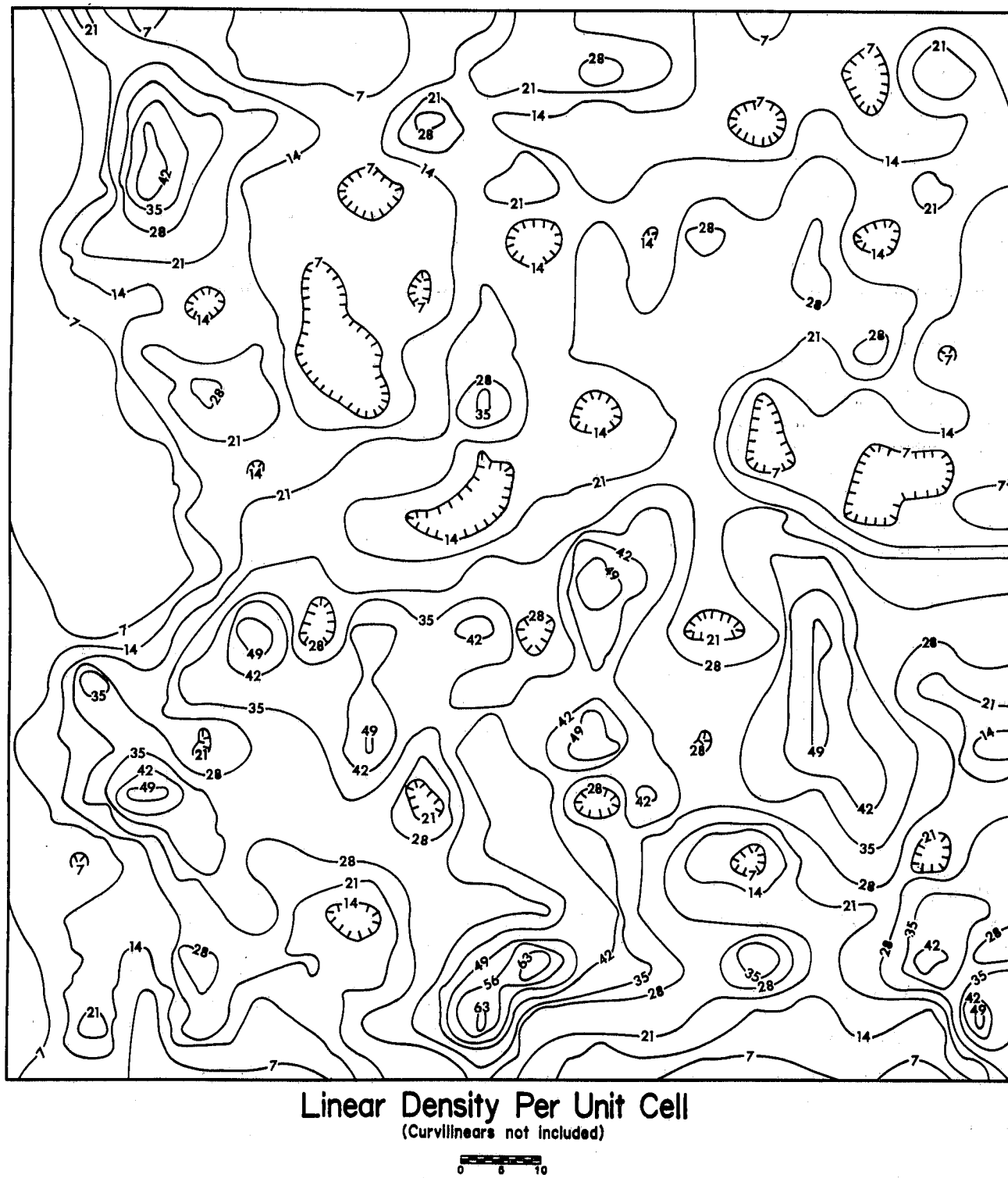

FIGURE 14.—*Linear density per unit cell contour map.*

sections (fig. 11). Generation of fracture permeability and positioning of the Altamont-Bluebell oil field are interpreted as a response to the interaction of the Towanta (Ritzma 1976) and the Strawberry Megalineaments (fig. 5). Megalineament intersections are also intimately associated with and surely a significant factor in the genesis of large annular structures (figs. 5, 6).

In the study area five megalineaments are involved in offset relationships. The remarkably straight course of megalineaments over tens of kilometers demonstrates their vertical orientation, and their persistence across geologic structures, geomorphic provinces, and drainage basins suggests some level of continuous activity. Consequently, a basement-generated wrench fault system has been postulated (Hodgeson 1976, Smith 1978, Abdel-Gawad and others 1976, Stone 1969, Morris and others 1964, Moody and Hill 1956, Moody 1966, Vening 1947. Not all megalineaments offset other megalineaments; however, Stone (1969) describes why in areas of thick sediment accumulation, because of subsurface zones of uncoupling, basement-derived wrench faulting is not necessarily exposed at the surface.

In the study area, annular structures are widely distributed with larger ones consistently associated with megalineament or large lineament intersection (figs. 3, 5, 6). Interpretation of these features is, at the present time, necessarily speculative.

Smith (1976) has proposed five separate possibilities of origin: (1) impact structures in basement which influence younger structures through tectonic heredity (Gallant 1963, Cohenour and Sharp 1968); (2) doming resulting from igneous intrusion and consequent collapse, as described by Longwell (1948) and Makin (1960); (3) drag folds along major strike-slip faults (Albers 1967); (4) tectonic heredity from circular features in basement which Fyfe (1974) proposes are the result of Archean convection cells—50 to 100 km in diameter; (5) a response to radial spreading from intrusion centers or the result of a buttressing effect of plutons or other rigid blocks.

To these possibilities I would add (1) a surface response through tectonic heredity of buried calderas; (2) piercement structures—especially the smaller ones (Moulton 1977); (3) rotational structures due to coupling stress at megalineament or lineament intersection as described by Emmons (1969); (4) surface response to cone fractures due to intrusion as reported by Bahat (1979); and (5) penetrative shattering of surface and subsurface rocks as the result of two intersection wrench faults as described by Lensen (1959) and Garfunkel (1966), resulting in more pervasive weathering and erosion in these areas.

Although separate annular structures may be the result of any or a combination of these possibilities, because large annular structures are consistently associated with megalineament intersection, and because of an apparent close relationship with drainage basins (fig. 2), I believe the latter reason to be the most important in this area.

Although more questions have arisen than have been addressed, let alone answered, in this study, it is obvious that remote sensing from space is an excellent reconnaissance tool, which, when utilized thoroughly, can be of great benefit to the industry in localizing prospective areas for more intensive investigation.

REFERENCES CITED

Abdel-Gawad, M., and Tubbesing, L., 1976, Transverse shear in southwestern North America—a tectonic analysis: In Hodgeson, R. A., Gay, S. P., and Benjamins, J. (eds.), Proceedings of the First International Conference on the New Basement Tectonics: Utah Geological Association Publication no. 5, p. 61–80.

Affleck, J., 1963, Magnetic anomaly trend and special patterns: Geophysics, v. 28, p. 379–95.

Albers, J. P., 1967, Belt of sigmoidal bending and right lateral faulting in the western Great Basin: Geological Society of America Bulletin, v. 78, p. 143–56.

Arabasz, W. J., Smith, R. B., and Richins, W. D., 1979, Earthquake studies in Utah, 1850 to 1978: University of Utah Seismograph Stations, Department of Geology and Geophysics, Special Publication.

Bahat, D., 1979, Interpretation on the basis of Hertzian theory of a spiral carbonate structure at Homa Mountain, Kenya: Tectonophysics, v. 60, p. 235–46.

Baker, A. A., 1964, Geologic map and sections of the Aspen Grove Quadrangle, Utah: U.S. Geological Survey, Geologic Quadrangle Map GQ-239.

———, 1964, Geologic map and sections of the Orem Quadrangle, Utah: U.S. Geological Survey, Geologic Quadrangle Map GQ-241.

———, 1972, Geologic map of the Bridal Veil Falls Quadrangle: U.S. Geological Survey, Geologic Quadrangle Map GQ-998.

———, 1973, Geologic Map of the Springville Quadrangle, Utah County, Utah: U.S. Geological Survey, Geologic Quadrangle Map GQ-1103.

———, 1976, Geologic map of the west half of the Strawberry Valley Quadrangle, Utah: U.S. Geological Survey Miscellaneous Investigations Map I-431.

Baker, A. A., and Crittenden, M. D., Jr., 1961, Geologic map of the Timpanogos Cave Quadrangle, Utah: U.S. Geological Survey Geologic Quadrangle Map GQ-132.

Baker, A. A., Calkins, F. C., Crittenden, M. D., Jr., and Bromfield, C. S., 1966, Geologic map of the Brighton Quadrangle, Utah: U.S. Geological Survey, Geologic Quadrangle Map GQ-534.

Bissell, H. J., 1952, Stratigraphy and structure of northeast Strawberry Valley Quadrangle, Utah: American Association of Petroleum Geologists Bulletin, v. 36, no. 4, p. 575–634.

Bromfield, C. S., Baker, A. A., and Crittenden, M. D., Jr., 1970, Geologic map of the Heber Quadrangle, Wasatch and Summit Counties, Utah: U.S. Geological Survey, Geologic Quadrangle Map GQ-864.

Bromfield, C. S., and Crittenden, M. D., Jr., 1971, Geologic map of the Park City East Quadrangle, Summit and Wasatch Counties, Utah: U.S. Geological Survey, Geologic Quadrangle Map GQ-852.

Bullock, K. C., 1962, Economic geology of north central Utah: Brigham Young University Geology Studies, v. 9, pt. 1, p. 85–93.

Cohenour, R. E., and Sharp, B. F., 1968, The impact theory: asteroids and the Earth-Moon system: Geo-Science News, v. 1, no. 3, p. 9–12.

Condie, K. C., 1969, Geologic evolution of the Precambrian rocks in northern Utah and adjacent areas: In Guidebook of northern Utah: Utah Geological and Mineralogical Survey Bulletin 82, p. 71–90.

Cook, K. L., Montgomery, J. R., Smith, J. T., and Gray, E. F., 1975, Simple Bouguer gravity anomaly map of Utah: Utah Geological and Mineral Survey Map 37.

Crittenden, M. D., Jr., 1965, Geology of the Draper Quadrangle, Utah: U.S. Geological Survey, Geologic Quadrangle Map GQ-377.

———, 1965, Geology of the Dromedary Peak Quadrangle, Utah: U.S. Geological Survey, Geologic Quadrangle Map GQ-378.

———, 1965, Geology of the Mount Aire Quadrangle, Salt Lake County, Utah: U.S. Geological Survey, Geologic Quadrangle Map GQ-379.

Crittenden, M. D., Jr., Calkins, F. C., and Sharp, B. J., 1966, Geologic map of the Park City West Quadrangle: U.S. Geological Survey, Geologic Quadrangle Map GQ-535.

El-Etr, H. A., 1976, Proposed terminology for natural linear features: In Hodgeson, R. A., Gay, S. P., Benjamins, J. (eds.), Proceedings of the First International Conference on the New Basement of Tectonics: Utah Geological Association Publication no. 5, p. 480–89.

Emmons, R. C., 1969, Strike-slip rupture patterns in sand models: Tectonophysics, v. 7, no. 1, p. 71–87.

Ericson, A. J., Jr., 1976, The Uinta-Gold Hill Trend: an economically important lineament: In Hodgeson, R. A., Gay, S. P., Benjamins, J. (eds.), Proceedings of the First International Conference on the New Basement Tectonics, Utah Geological Association Publication no. 5, p. 126–38.

Fyfe, W. S., 1974, Archean tectonics: Nature, v. 249, p. 000.

Gallacher, Mark H., 1975, Fractures and surface lineaments in northeastern Utah: Master's thesis, University of Utah, Salt Lake City.

Gallant, R. L. C., 1963, Meteorite impacts, lunar maria, lopoliths, and ocean basins: Nature, v. 197, p. 38–39.

Garfunkel, Z., 1966, Problems of wrench faults: Tectonophysics, v. 3, no. 5, p. 457–73.

Gay, S. P., 1972, Aeromagnetic lineaments: their geological significance and their significance to geology: American Stereo Map Company, Salt Lake City, Utah.

———, 1973, Pervasive orthogonal fracturing in Earth's continental crust; a closer look at the new basement tectonics: American Stereo Map Company, Salt Lake City, Utah.

Geologic Staff and Illustrations Section, Utah Geological and Mineral Survey (compilers), 1977, Energy resources map of Utah: Utah Geologic and Mineral Survey Map 44.

Glukhovskiy, M. Z., 1977, Ring structures and linear faults in the Aldan Shield and Stanovoy region (as interpreted from satellite photographs): Geotectonics, v. 10, no. 5, p. 326–32.

Heylmun, E. B., 1959, The ancestral Rocky Mountain system in northern Utah: In Guidebook to the geology of the Wasatch and Uinta Mountains transition area: Intermountain Association of Petroleum Geologists Guidebook, 10th Annual Field Conference, p. 172–74.

Hilpert, L. A., and Roberts, R. J., 1969, Economic geology: In Mineral and water resources of Utah, Reports of the U.S. Geological Survey and the Utah Geological and Mineral Survey: 91st Congress, First Session, p. 28–38.

Hintze, L. F., 1973, Geologic history of Utah: Brigham Young University Geology Studies, v. 20, pt. 3, 181p.

———, 1980, Geologic map of Utah: Utah Geological and Mineral Survey, 1:500,000.

Hodgeson, R. A., 1976, Review of significant early studies in lineament tectonics: In Hodgeson, R. A., Gay, S. P., Benjamins, J. (eds.), Proceedings of the First International Conference on the New Basement Tectonics: Utah Geological Association Publication no. 5, p. 1–10.

Johnson, A. C., 1976, Lineament analysis: an exploration method for the delineation of structural and stratigraphic anomalies: In Hodgeson, R. A., Gay, S. P., Benjamins, J. (eds.), Proceedings of the First International Conference on the New Basement Tectonics: Utah Geological Association Publication no. 5, p. 449–52.

Kelley, V. C., 1955, Regional tectonics of the Colorado Plateau and relationship to the origin and distribution of uranium: University of New Mexico Publications in Geology, no. 5, 120p.

———, 1960, Fracture systems and tectonic elements of the Colorado Plateau: University of New Mexico Publications in Geology, no. 6, 104p.

King, P. B., 1969, Tectonic map of North America: U.S. Geological Survey, scale 1:5,000,000.

———, 1977, The evolution of North America: Princeton University Press, Princeton, New Jersey, 197p.

Lensen, G. U., 1959, Secondary faulting and transcurrent splay faulting at transcurrent fault intersections: New Zealand Journal of Geology and Geophysics, v. 2, p. 729–34.

Levandowski, D. W., Jennings, T. V., Lehman, W. T., 1976, Relations between ERTS lineaments, aeromagnetic anomalies, and geologic structures in north central Nevada: In Hodgeson, R. A., Gay, S. P., Benjamins, J. (eds.), Proceedings of the First International Conference on the New Basement Tectonics: Utah Geological Association Publication no. 5, p. 106–17.

Longwell, C. R., 1948, Low-angle normal faults in the Basin and Range Province: American Geophysical Union Transactions, v. 26, pt. 1, p. 107–18.

Mabey, D. R., Crittenden, M. D., Jr., Morris, H. T., Roberts, R. J., and Tooker, E. W., 1964, Aeromagnetic and generalized geologic map of part of north central Utah: U.S. Geological Survey Geophysics Investigations Map GP-422.

Makin, J. Y., 1960, Structural significance of tertiary volcanic rocks in southwestern Utah: American Journal of Science, v. 258, no. 2, p. 81–131.

Moody, J. D., 1966, Crustal shear patterns and orogenesis: Tectonophysics, v. 3, no. 6, p. 479–522.

Moody, J. D., and Hill, M. J., 1956, Wrench fault tectonics: Geological Society of America, v. 67, p. 1207–46.

Morris, H. T., and Shepard, W. M., 1964, Evidence for a concealed tear fault with a large displacement in the central east Tintic Mountains, Utah: U.S. Geological Survey Professional Paper 501-C, p. C19–C21.

Moulton, F. D., 1977, Lower Mesozoic and upper Paleozoic petroleum potential of the hingeline area, central Utah: Brigham Young University Geology Studies, v. 24, pt. 1, p. 1–10.

Osmond, J. C., 1965, Geologic history of site of Uinta Basin, Utah: American Association of Petroleum Geologists Bulletin, v. 49, no. 11, p. 1957–73.

Peterson, R. M., 1976, Curvilinear features visible on small-scale imagery as indicators of geologic structures: In Hodgeson, R. A., Gay, S. P., Benjamins, J. (eds.), Proceedings of the First International Conference on the New Basement Tectonics: Utah Geological Association Publication no. 5, p. 618–25.

Raisz, E. J., 1945, The Olympic-Wallowa Lineament: American Journal of Science, v. 243-A, Daly Volume, no. 2, p. 479–85.

———, 1957, Map of the landforms of the United States, 6th revised edition: To accompany Atwood, W. W., Physiographic provinces of North America, 1940.

Ritzma, H. R., 1969, Tectonic resumé, Uinta Mountains: In Geologic guidebook of the Uinta Mountains, Intermountain Association Geologists Sixteenth Annual Field Conference.

———, 1976, Towanta Lineament, northern Utah: In Hodgeson, R. A., Gay, S. P., Benjamins, J. (eds.), Proceedings of the First International Conference on the New Basement Tectonics: Utah Geological Association Publication no. 5, p. 118–25.

Roberts, R. J., 1960, Alineament of mining districts in north central Nevada: U.S. Geological Survey Professional Paper 400-B, p. 17–19.

Runyon, D. M., 1977, Structure, stratigraphy, and tectonic history of the Indianola Quadrangle, central Utah: Brigham Young University Geology Studies, v. 24, pt. 2, p. 63–79.

Salas, G. P., 1977, Relationship of mineral resources to linear features in Mexico as determined from Landsat data: In Woll, P. W., and Fisher, W. A. (eds.), Proceedings of the First Annual William T. Pecorah Memorial Symposium: U.S. Geological Survey Professional Paper 1015, p. 61–73.

Smith, M. R., 1976, Arcuate structural trends and basin and range structures, In Hodgeson, R. A., Gay, S. P., Benjamins, J. (eds.), Proceedings of the First International Conference on the New Basement Tectonics, Utah Geological Association Publication no. 5, p. 626–34.

Smith, R. B., 1978, Intraplate tectonics of interior of western Cordillera: Geological Society of America Memoir 152: Cenozoic tectonics and regional geophysics of the western Cordillera, p. 111–44.

———, 1978, Fault-plane solutions of the western United States: a compilation: Cenozoic tectonics and regional geophysics of the western cordillera: Geological Society of America Memoir 152, p. 107–9.

Stokes, W. L., 1977, Subdivisions of the major physiographic provinces in Utah: In Utah Geology, Spring 1977, v. 4, no. 1.

Stone, D. S., 1969, Wrench faulting and Rocky Mountain tectonics: Wyoming Geological Association Earth Science Bulletin, p. 27–41.

———, 1974. Lineaments: their role in tectonics of central Rocky Mountains: a discussion: The Wyoming Geological Association Earth Science Bulletin, v. 7, no. 4, p. 1–11.

Taranik, J. V., 1978, Characteristics of the Landsat multispectral data system: U.S. Geological Survey Open File Report 76-402, 75p.

———, 1978, Computer processing of geologic applications: U.S. Geological Survey Open File Report 78-117, 50p.

Taranik, J. V., and Trautwein, C. M., 1976, Integration of geological remote-sensing techniques in subsurface analysis: U.S. Geological Survey Open File Report 76-402, 60p.

Vening Meinesz, F. A., 1947, Shear patterns of the earth's crust: American Geophysical Union Transactions, v. 28, no. 1, p. 1–61.

Warner, M. M., 1980, Southern Idaho, northern Nevada, southeastern Oregon—prime exploration target: Oil and Gas Journal, v. 78, no. 18, p. 325–41.

Young, G. E., 1976, Geology of Billies Mountain Quadrangle, Utah County, Utah: Brigham Young University Geology Studies, v. 23, pt. 1, p. 205–80.

Zietz, I., Bateman, P. C., Case, J. E., Crittenden, M. D., Jr., Griscom, A., King, E. R., Roberts, R. J., and Lorentzen, G. R., 1969, Aeromagnetic investigations of crustal structure for a strip across the western United States: Geological Society of America Bulletin, v. 80, p. 9, p. 1703–14.

Zietz, I., Shuey, R., and Kirby, J. R., Jr., 1976, Aeromagnetic map of Utah: U.S. Geological Survey Geophysical Investigations Map GP-907.